

Temporal variations in the chemical composition of aerosols over the coastal Bay of Bengal

V. R. Kumari¹, V.V.S.S. Sarma^{1,2,*}, G. Mahesh³ and A.K. Sudheer³

¹CSIR-National Institute of Oceanography, 176 Lawsons Bay Colony, Visakhapatnam, India

²Academy of Scientific and Innovative Research, Gaziabad, India

³Physical Research Laboratory, Ahmedabad, India

*Corresponding author: sarmav@nio.org

Abstract

Variations in source, ionic composition and carbonaceous components of aerosols are expected in the atmosphere due to reversing the direction of winds from winter to summer over the coastal Bay of Bengal (BoB). To examine this monthly, samples were collected at the weekly interval between March 2016 and February 2017 in the coastal BoB. The air mass back trajectories suggested that the study region received aerosols from Indo-Gangetic Plain from October to February whereas from central India during June to September and south or southwest during March to May. A higher concentration of total suspended particulate matter (TSP) was observed from November to February (winter) compared to other months. The concentration of sulphate contributed more than half of water-soluble inorganic species followed by sodium, ammonium and nitrate. The dominant contribution of anthropogenic SO_4^{2-} (>90%) to total SO_4^{2-} was observed. The ambient elemental carbon loadings and organic carbon to EC ratios indicate the dominant contribution of biomass burning emissions in the study region. The significant contribution of non-sea salt sulphate and nss-K^+ indicates a dominant contribution from the continental sources throughout the year. The mass ratio of $\text{NO}_3^-/\text{anthropogenic SO}_4^{2-}$ suggests stationary sources (i.e., coal burning in power plants) contribute significantly over vehicular emissions during the entire study period. The mass balance of ionic composition suggests the acidic nature of aerosols. The estimated secondary aerosols accounted for ~50% of organic carbon and 7% of TSP in the study region. This study has implications for understanding the source, composition and nature of aerosols and possible impacts on coastal water upon its deposition.

Keywords: Total suspended particles; biomass burning, Indo-Gangetic Plain; time-series; Bay of Bengal.

1. Introduction

The total suspended particulate matter (TSP) in the atmosphere significantly influences the local climate through modifications in the radiation budget and cloud properties (Andrea and Ramanathan, 2013; Hu et al., 2017). The rapid increase in aerosol emissions from South and Southeast Asia since the middle of 1990 is a major concern due to rapid industrialization and population growth (Kurokawa and Ohara, 2020). Several investigators noticed that carbonaceous aerosols have a significant impact on several extreme climatic conditions such as storms, droughts, and delay in onset of monsoon, rainfall pattern etc. (Seinfeld et al., 2004; Fadnavis et al., 2019). Significant uncertainty exists on assessment of the impact of aerosols on the climatic events due to lack of information on the chemical composition of aerosols, especially organic aerosols, as they have a significant impact on regional radiative forcing (Gogoi et al., 2017).

Carbonaceous aerosols, both elemental carbon (EC) and organic carbon (OC) control the earth's radiation budget. The net effect on radiation depends on the ratio of EC to OC and there are large uncertainties in the models due to lack of enough data (Cooke et al., 1999; Bond et al., 2004). EC is also known to absorb trace gases such as NO_x , SO_2 and O_3 and enhances several chemical reactions in the atmosphere (Gundel et al., 1989). The rapid industrialization and urbanization in South and Southeast Asia (Kurokawa and Ohara, 2020) may lead to possible enhancement in the release of carbonaceous aerosols into the atmosphere (Cooke et al., 1999). The major source of EC and OC comes from vehicular exhaust, biomass burning, sea-salt aerosols, power plants and industrial emissions. Choo Chuay et al. (2020) found that both vehicular exhausts and biomass burning are the major source of ambient air in Bangkok. Based on the OC/EC and OC/ K^+ ratio, Bhowmik et al. (2020) identified the dominance of biomass burning from wood fuel and agricultural waste in the Indo-Gangetic Plain (IGP) region. Similarly, Flores et al. (2020) found that the major source of OC/EC in Istanbul comes from fossil fuel used for residential heating and vehicular emissions. Jafar and Harrison (2020) found a significant increasing trend in carbonaceous aerosols from rural to urban areas in the UK and mainly attributed to regional transport.

Besides climatic influence, aerosols are a significant source of nutrients to oceans (Jickells et al., 2005; Mahowald et al., 2010; Ma et al., 2021; Ventura et al., 2021). The continental aerosols, including anthropogenic aerosols, get transported over the ocean under conducive meteorological conditions, and their deposition modifies primary production (Srinivas et al., 2011; Maranen et al., 2010), phytoplankton composition (Yadav et al., 2016) and ocean acidification (Doney et al., 2007; Sarma et al., 2015; Kumari et al., 2021; Sarma et al., 2021). The deposition of aerosols depends on the strength of emission, the distance from the source and the meteorological conditions (wind speed, direction).

These factors have significant temporal and spatial variability. Since the monsoonal system exists in the south and Southeast Asia lead to a seasonal reversal in direction wind with variable intensity in wind speed that modifies source and depositional velocity of the aerosols over the northern Indian Ocean. Due to intense anthropogenic activities in the south and southeast Asia, with a seasonal reversal in wind direction, large temporal variability in the aerosol composition is anticipated in this region.

India is the second-largest anthropogenic aerosol emitting country in the world (Kurokawa and Ohara, 2020) with a significant impact on the climate of Asia (Ji et al., 2011). Several studies have been conducted to evaluate the composition of aerosols from urban/semi-urban regions in India (Kulshrestha et al., 1998; Momin et al., 1999; Ramachandran, 2005) but limited studies were carried out in the rural or remote regions (eg: Mahadevan et al., 1989). Ramanathan et al. (2001) demonstrated the importance of aerosols emitted from the land on the Indian Ocean and the regional hydrological cycle.

The northeastern Indian Ocean (Bay of Bengal; BoB) is landlocked in the north, east and western sides and opened to the south to the Indian Ocean. Winds blow from the northeast during winter and southwest during summer. Higher levels of both total and anthropogenic AOD were reported along with the northwestern and western coastal BoB with a higher rate of increase over the past two decades (Yadav et al., 2021). Sudheer and Sarin (2008) found that higher abundances of EC during winter due to the strong influence of polluted air mass from the Indo-Gangetic Plain (IGP) and its influence decreases during spring due to change in direction of the wind. Several investigators measured carbonaceous aerosols in the IGP region where biomass burning, vehicular exhaust and agricultural waste and also through formation of secondary aerosols were found to be significant contributors during winter and post-monsoon seasons (Satsangi et al., 2010; Ram et al., 2010; Ram and Sarin, 2015; Bhowmik et al., 2020). The transport of pollutant aerosols and their composition during winter and summer were reported over the BoB (Kumar et al., 2008; Srinivas et al., 2011) based on one-time measurements onboard research vessels. These studies highlighted the differences in source regions and nature of aerosols between the Arabian Sea and BoB. A few studies were carried to evaluate the chemical composition of inorganic constituents in the aerosols in the coastal cities of India (Jose et al., 2019; Ramachandran, 2005), however, studies on carbonaceous aerosol are rather very few (Kommula et al., 2021).

The previous investigations suggested that dominant anthropogenic source emissions on the marine atmospheric boundary layer (MABL) of the BoB compared to the Arabian Sea (Kumar et al., 2008; Srinivas and Sarin, 2012) based on the chemical composition of the aerosols collected over the basin during different seasons onboard research vessel. This gives a snapshot of information and represents

the compositional characteristics of marine aerosols under different pollution regimes. However, a comprehensive study with sufficient time resolution to assess the seasonal variability in aerosol composition and its dependence on meteorological conditions are rather limited for this region. Yadav et al. (2016) reported that that 60-70% of the TSP over the coastal city, Visakhapatnam, is deposited in the coastal BoB that enhances surface ocean primary production and acidification (Sarma et al., 2021). Since the direction of the winds changes with the season due to the northeast (winter) and southwest (summer) monsoons, the source and chemical composition of the aerosols are expected to be different. Hence, TSP samples were collected at a weekly interval for a period of one year at a fixed coastal station to examine the seasonal variability in the chemical composition of aerosols (carbonaceous species and water-soluble inorganic species). The objective of this study is to 1) assess the seasonal variability in mass concentrations of carbonaceous and water-soluble inorganic species over the coastal BoB, 2) identify seasonal variability in the source of aerosols through diagnostic mass ratios in the coastal BoB and 3) evaluate the nature of aerosols (acidic versus basic) over the coastal BoB and examine the potential sources responsible for their nature.

2. Material and methods

The sampling location, Visakhapatnam (17.62°N and 83.22°E; Fig. 1) is a moderate city, houses many major industrial activities. The National Thermal Power Plant (NTPC) is located about 30 km east of the study region. The studies on aerosols in this region were mainly concentrated to understand the radiation budget, and air pollution with meteorological conditions (Niranjan et al., 2007; 2011; Rao and Niranjan, 2012).

2.1. Collection of TSP samples

TSP samples were collected from March 2016 to February 2017 from the terrace of the CSIR-National Institute of Oceanography, Visakhapatnam building at a height of ~20 m above the mean sea level. Meteorological data were obtained using Automatic Weather Stations (AWS) installed close to aerosol sampling location. The air mass back trajectories (AMBTs) were drawn to identify both the source region and route of transport to the study region (Fig. 1). Using the Global Data Assimilation System (GDAS) database (National Oceanic and Atmospheric Administration (NOAA)) and the Hybrid Single-Particle Lagrangian Integrated Trajectory Model (HYSPLIT program, version 4.0, <http://ready.arl.noaa.gov/HYSPLIT.php>), the wind back trajectories were computed (Draxler, 1999). The weekly AMBT were prepared and presented in Figure 1. The monthly mean MODIS AOD (level 3) data were obtained from (<https://ladsweb.modapseosdis.nasa.gov/search>). ERA-Interim reanalysis

of monthly wind speed at 10 m height from the surface and wind vectors data with a resolution of 1 x 1° grid was downloaded from <https://giovanni.gsfc.nasa.gov/giovanni>.

2.2. Measurement of ionic composition of TSP

TSP aerosols were collected on pre-combusted quartz (PALLFLEX, 8”x10”) filters. The aerosols deposited on the filter was determined gravimetrically using an electronic balance (Sartorius MF 5). The filter was subsampled (47mm hole punch) and kept in the beaker containing 50 ml of Milli-Q water and sonicated for 30 min. The extract was centrifuged at 2000 rpm for 30 minutes and transferred to clean Teflon tubes and subjected to ion chromatography for measurement of ionic composition. The anions (F⁻, Cl⁻, SO₄²⁻, NO₃⁻) and cations (NH₄⁺, Na⁺, K⁺, Ca²⁺ and Mg²⁺) were measured by ion chromatography (IC; 85- Professional IC, M/s Metrohm, Switzerland). The mixture of 3.2 mM Na₂CO₃, 1 mM NaHCO₃, and 0.1 mM H₂SO₄ are used as an eluent for anions whereas 2 mM HNO₃ for cations. Filter blanks were analyzed and the same is subtracted from the sample. About 20 µl of the aerosol extract is injected into the anion/cation column for measurements of elemental concentrations. The instrument was calibrated using multi-anion and cation standards (Sigma-Aldrich, S.No. 69734, 91286). The precision in the measurements was found to be <10% based on repeat analysis of the same sample. Several samples were spiked with a known concentration of ionic species to quantify recovery and it is in the range of 87 to 110% for the ions measured. The relative standard deviation of each ion was less than 5% of the mean concentration. The detection limit for anions and cations was 0.05 and 0.008 mg/l respectively.

Using the formulae given by Keene et al (1986), the non-sea salt (nss) components were estimated:

$$\text{nss-K}^+ = \text{K}^+ - 0.037 * \text{Na}^+$$

$$\text{nss-Ca}^{2+} = \text{Ca}^{2+} - 0.038 * \text{Na}^+$$

$$\text{nss-Mg}^{2+} = \text{Mg}^{2+} - 0.12 * \text{Na}^+$$

$$\text{nss-SO}_4^{2-} = \text{SO}_4^{2-} - 0.25 * \text{Na}^+$$

where 0.037, 0.038, 0.12 and 0.25 denotes weight ratios of K⁺, Ca²⁺, Mg²⁺ and SO₄²⁻ to Na⁺ in seawater respectively and K⁺, Ca²⁺, Mg²⁺ and SO₄²⁻ represent concentrations in aerosols.

2.3. Measurements of carbonaceous components

A subsample of 1.5 cm² area from the sample filter was taken for the analysis of carbonaceous species, elemental carbon (EC) and organic carbon (OC) using EC-OC analyzer (Sunset Laboratory, SF, CA) following the NIOSH-5040 Total Optical Transmission (TOT) protocol (Birch and Carry, 1996; Ram et al., 2010; Xu et al., 2017). The accuracy of the instrument was determined using sucrose and

potassium hydrogen phthalate standards. No detectable procedural blanks were observed for EC. On the other hand, the procedural blank for OC was found to be <10%. The precision of the EC and OC analysis was 10 and 5% respectively based on the repeat analysis of the same sample. The concentration of particulate organic matter (POM) is computed as 1.6 times of OC. The concentration of water-soluble organic carbon (WSOC) was analyzed by extracting organic carbon in the 10 cm² of filter in the MilliQ water by ultrasonication and the non-purgeable organic carbon (NPOC) was measured using total organic carbon analyzer (TOC analyser (isoTOC), M/s Elementaar analytical, Germany). The calibration of the TOC analyser was done using the potassium hydrogen phthalate standard. The replicate analysis of filter samples yielded ~5% of WSOC.

2.4. Estimation of neutralization potential to acidic potential

The ratio of Neutralization Potential to Acidic Potential (NP/AP) and total hydrogen ion available was computed following equations given by Yadav et al. (2019)

$$\text{NP/AP} = ([\text{NH}_4^+] + [\text{Na}^+] + 2*[\text{Ca}^{2+}] + 2*[\text{Mg}^{2+}] + [\text{K}^+]) / (2*[\text{SO}_4^{2-}] + [\text{NO}_3^-] + [\text{Cl}^-]) \text{ -- (1)}$$

and

$$[\text{H}^+]_{\text{T}} = (2*[\text{SO}_4^{2-}] + [\text{NO}_3^-] + [\text{Cl}^-] - [\text{NH}_4^+] - [\text{Na}^+] - 2*[\text{Ca}^{2+}] - 2*[\text{Mg}^{2+}] - [\text{K}^+]) \text{ --- (2)}$$

3. Results and Discussion

3.1. Air-mass back trajectories in the marine atmospheric boundary layer (MABL)

Air mass back trajectories suggested that the study region received aerosols from the southwest region (south India) from March to May and from the western region (i.e., western and central India) from June to October and northeast region (mostly Indo-Gangetic Plain (IGP)) during winter (November to February) (Fig. 1). The change in direction of the source of aerosol is driven by a seasonal reversal in winds caused by monsoonal circulation (Schott and McCreary, 2001). As a result, the abundance and composition of TSP are expected to show significant temporal variability over the coastal BoB.

3.2. Temporal variability in ionic species in the TSP over the coastal BoB

The concentration of TSP over the coastal BoB varied between 8.8 and 177.3 (mean of 75.3) $\mu\text{g m}^{-3}$ (Table 1) with higher concentrations during October to February ($112 \pm 26 \mu\text{g m}^{-3}$) and lower during March to September ($58.8 \pm 8 \mu\text{g m}^{-3}$) (Fig 2a). Water-soluble inorganic solids (WSIS) in TSP over the coastal BoB also displayed similar temporal variability (Fig. 2b). Following Keene et al. (1986) method, the aerosol concentrations of K^+ , Ca^{2+} and SO_4^{2-} were corrected to remove sea-salt contribution using the Na^+ levels in the TSP to separate anthropogenic fraction. The higher concentrations of sea-salt components, such as Na^+ , Cl^- and Mg^{2+} , were observed during May to June

and November to February (winter) compared to other months (Fig. 3a-c). On the other hand, the higher loadings of anthropogenic components, such as NH_4^+ , nss-K^+ and nss-SO_4^{2-} were noticed during winter compared to other months (Fig. 3d-f) suggesting the dominant source of anthropogenic contribution during this period. Higher contribution of water-soluble K^+ and SO_4^{2-} can be sourced from biomass burning and coal combustion respectively to the TSP (Srinivas and Sarin, 2014). The contribution of SO_4^{2-} was dominant and contributed to 24-56% of total ions measured with $>\sim 40\%$ contribution during all months except March and May (Fig. 4). After SO_4^{2-} , Na^+ was the dominant contributor (12-29%) followed by Cl^- (7-17%), NO_3^- (3-10%). The contribution of Ca^{2+} was higher during April to October (10-25%) whereas it was low (1-6%) during other months (Fig. 4). The significant contribution of nss-SO_4^{2-} (anthropogenic SO_4^{2-}) (63-84%) to total SO_4^{2-} whereas biogenic SO_4^{2-} and sea-salt SO_4^{2-} contributed 7 to 10% and 6-30% respectively (Supplementary Fig S1). Similarly, a high contribution of nss-K^+ (48-88%) to bulk K^+ (0.2 to $2.9 \mu\text{g m}^{-3}$) was observed in the coastal BoB indicating that dominant contribution from the continental sources throughout the year (Fig. 4). The higher contribution of K^+ , SO_4^{2-} , NH_4^+ during October to February (2-6%, 40-56% and 2-22%) suggest that significant amounts of anthropogenic pollutants transported from IGP to the study region when wind blow from north/northeast direction (Fig. 1 and 4). The concentration of Ca^{2+} was higher during April to June and November ($>2 \mu\text{g m}^{-3}$) compared to other months ($<1 \mu\text{g m}^{-3}$) suggesting the higher contribution of anthropogenic aerosols during the latter period (Fig. 3g). The higher contribution of Ca^{2+} was found during March to October (10-25%) than other months (1-4%) suggesting dominant natural sources during the former period (Fig. 4). The major source of Ca^{2+} mineral dust to the study region comes from the Thar desert in northwestern India and the middle east (Rastogi and Sarin, 2006; Kumar and Sarin, 2009). The concentration of NO_3^- increases steadily from March to October and decreased to February (Fig 3h). The contribution of NO_3^- was higher during March to October (5-10%) compared to other months (3-4%) suggesting that aerosols from central and western India contributes significantly than IGP (Fig. 4). The higher concentrations of both nss-Ca^{2+} and NO_3^- were noticed during March to October in the TSP over the coastal BoB than those of other months and this co-occurrence may be caused by heterogeneous uptake of HNO_3 by the mineral dust in the coarse mode particles (Kumar et al., 2008a; Cruz et al., 2019; Bikkina et al., 2020). In summary, the ionic composition of TSP suggests the dominant contribution of continental sources over the coastal BoB throughout the year with a higher contribution during winter than other seasons.

3.3. Temporal variability in carbonaceous components over the coastal BoB

The average EC concentration in the MABL of coastal BoB was $1.8 \mu\text{g m}^{-3}$ (range: 0.4 to $4.7 \mu\text{g m}^{-3}$) during the study period with higher concentrations during winter ($2.1 \pm 0.2 \mu\text{g m}^{-3}$) and lower during

other months ($1.6 \pm 0.3 \mu\text{g m}^{-3}$) (Fig. 3i). The concentration of EC in the study region is much less than that observed in northeastern India ($0.6\text{-}12.6 \mu\text{g m}^{-3}$; Bhowmik et al., 2020) and the urban region in the UK ($0.5\text{-}15 \mu\text{g m}^{-3}$; Jafar and Harrison, 2020) but close to that of the northeastern and northwestern IGP ($1.9\text{-}5.8 \mu\text{g m}^{-3}$; Ram et al., 2010; Singh et al., 2016), Istanbul city ($1\text{-}4.5 \mu\text{g m}^{-3}$; Flores et al., 2020). EC displayed a significant linear relationship with TSP ($r^2=0.29$; $p<0.001$; Table 2) during the entire study period. The contribution of EC to the TSP ranged between 1.6 and 4.2% with an average contribution of $2.5 \pm 0.6\%$ and it is almost close to that reported in the entire BoB (2%; Sudheer and Sarin, 2008) and IGP region (Ram et al., 2010). The mass fraction of EC to TSP is lower during winter ($1.9 \pm 0.4\%$) due to the higher concentration of both TSP and EC compared to other months ($2.7 \pm 0.6\%$). This temporal difference could be due to the variable contribution of aerosols from the IGP region and also coarser/fine particles (mineral dust and/or sea salt) that modifies the contribution of EC to the TSP. EC is mostly confined to the smaller size particles, and their contributions may be decreased from coastal and open sea regions due to long-range transport (Sudheer and Sarin, 2008). The mean EC in the coastal BoB ($1.8 \pm 0.4 \mu\text{g m}^{-3}$) in this study is higher than reported over the entire BoB ($0.4 \mu\text{g m}^{-3}$; Sudheer and Sarin, 2008) and Arabian Sea ($1.4 \pm 0.5 \mu\text{g m}^{-3}$; Bikkina et al., 2020) but close to that reported in the Arabian Sea by Kumar et al. (2012; $2.2 \mu\text{g m}^{-3}$). The mean EC in the coastal BoB is much lower than the same found in the western IGP region (0.5 to $12.5 \mu\text{g m}^{-3}$; Bhowmik et al., 2020) and eastern IGP ($1.9\text{-}5.8 \mu\text{g m}^{-3}$; Ram et al., 2010) with higher concentrations during winter and lower during summer. A significant decrease in EC concentrations in the study region may be caused by dilution in the en-route.

The concentration of OC ranged between 2.8 and $19.2 \mu\text{g m}^{-3}$ with a mean of $11.5 \pm 4 \mu\text{g m}^{-3}$ in the coastal BoB (Fig. 3j) and it is significantly higher than that reported in the open BoB (0.3 to $5.5 \mu\text{g m}^{-3}$; Sudheer and Sarin, 2008) and Arabian Sea (3.0 to $9.8 \mu\text{g m}^{-3}$; Kumar et al., 2012; Srinivas and Sarin, 2013; Bikkina et al., 2020; Ashwini et al., 2020) due to proximity to the source region in the present study. It can be noted that the concentration of OC is higher in the eastern and western IGP ($12.8\text{-}80.4 \mu\text{g m}^{-3}$; Ram et al., 2010; Bhowmik et al., 2020), Dhaka, Bangladesh ($45.7 \pm 10 \mu\text{g m}^{-3}$; Salam et al., 2003), Karachi, Pakistan ($39.9 \pm 22.8 \mu\text{g m}^{-3}$; Chen et al., 2019), Katmandu, Nepal ($34.8 \pm 27.1 \mu\text{g m}^{-3}$; Chen et al., 2019) than our study region but close to that of Beijing, China ($11 \pm 10.7 \mu\text{g m}^{-3}$; Ji et al., 2019; Tang et al., 2018), Sao Paulo, Brazil ($6.7\text{-}2.7 \mu\text{g m}^{-3}$; Monteiro dos Santos et al., 2016; Martins Pereira et al., 2017). In addition to this, interannual variability in winds, rate of emission and its transport contributed significantly to the large variability in the carbonaceous components reported earlier and in the present study. The temporal variability in OC follows that of TSP with higher levels

during winter ($15.3 \pm 4 \mu\text{g m}^{-3}$) than other months ($9.6 \pm 2 \mu\text{g m}^{-3}$; Fig 2a, and 3j). The computed POM contributed to 10 to 31% of the TSP with a mean of $18 \pm 6\%$ in the coastal BoB. The higher contribution of POM to TSP was observed during winter ($25 \pm 6\%$) when the study region received aerosols from IGP than other months ($15 \pm 3\%$) suggesting that aerosols from IGP contribute a significant fraction of POM to TSP.

The source of EC and OC were different as EC primarily originates from anthropogenic sources, such as combustion of biomass or fossil fuel, whereas OC is produced along with EC as well as biogenic and secondary processes from the precursor gases (Sun and Arya, 2006). The nature of carbonaceous aerosols in the atmosphere can be evaluated from the relationship between OC and EC. The significant linear relationship between OC and EC was observed during all months ($r^2=0.71$; $p<0.001$; Table 2), except winter, when it displayed negative relation ($r^2=0.44$; $p<0.001$; Table 2; Fig. 5a) suggesting the primary nature of the OC in this region during the former period. The inverse correlation during winter may be caused by preferential removal of one component over the other during transport due to the difference in the lifetime of EC and OC in the atmosphere (Lim et al., 2003). In contrast, the OC/EC ratio was higher during winter (8.3 ± 2) than other months (5.8 ± 0.9) and it is due to the higher contribution of OC as well as EC from the IGP region. On the other hand, a significant decreasing trend in the concentration of OC and OC/EC ratios were found from north to south of BoB and attributed to a higher rate of removal of OC than EC (Sudheer and Sarin, 2008). Similar EC/OC ratios were observed in northern India (4.4 to 8.5; Bhowmik et al., 2020; Rengarajan et al., 2007; Sharma et al., 2014; Ram and Sarin, 2010). The lower OC/EC ratios (1.7-4.2) than present study region was observed in Brazil (Sao Paulo), China (Beijing), Bangladesh (Dhaka) and Nepal (Salam et al., 2003; Chen et al., 2019; Ji et al., 2019; MartinsPereira et al., 2017). Based on field experiments, Lim et al. (2003) confirmed the longer residence time of EC than OC over the Asian atmosphere and it is depended on the particle size, volatility, reactivity and scavenging efficiency. Since several volatile or semi-volatile species contribute to OC, whereas EC is mainly contributed by non-volatile and stable species, the scavenging of OC is expected to be higher than EC. In addition to this, a significant fraction of OC is water-soluble as a result it undergoes hygroscopic growth and removal from the atmosphere (Decesari, 2001). Nevertheless, the OC/EC ratios in the study region (2.9 to 15.7) suggests biomass burning than the contribution of emissions from light and heavy-duty vehicles (0.6-1.9) at Sao Paulo, Brazil (Monteiro dos Santos et al., 2016). Several investigators reported high OC/EC ratios for biomass burning and lower for vehicular emissions (Andreae and Merlet, 2001; Ram et al., 2010; Sandradewi et al., 2008). The seasonal variations in OC/EC ratios may be caused by temporal variations in emission characteristics or the type of biomass burning associated with meteorological conditions

(Hopkins et al., 2007). In addition to this removal of semi-volatile species during sampling may also modify OC/EC ratios (Viana et al., 2006).

The ratio of water-soluble (WSOC) to water-insoluble organic carbon (WIOSC/WIOC) indicates the processing of organic carbon through photochemical reactions during their transport (Sullivan and Weber, 2006; Favez et al., 2008). The concentration of WOSC and WIOC were ranged from 3.3 to 5.8 (mean of $4.5 \pm 0.7 \mu\text{g m}^{-3}$) and 2.2 to 13.43 (mean of $7.0 \pm 3 \mu\text{g m}^{-3}$) respectively with relatively higher during October to December in the coastal BoB. The OC and WSOC displayed significant linear relation and the slope suggested that about 16% of OC is contributed by WSOC (Fig. 5b: Table 2). The mean WSOC/OC ratio was lower during winter (0.3 ± 0.04) than other months (0.5 ± 0.1) suggesting the lower contribution of WSOC to OC during the former period. Relatively higher ratios of WSOC/OC were reported in the IGP region (0.6-0.9; Bhowmik et al., 2020) than the present study region indicating a contribution from secondary organic aerosols (SOA) or ageing of the aerosols during transport (Pio et al., 2007). Several studies suggested that organic carbon sourced from vehicular exhaust produce low WSOC/OC ratio than biomass burning due to the generation of less soluble organic constituents due to the combustion of fuels (Daellenbach et al., 2016; Ram et al., 2012; Cheung et al., 2009). Dallenbach et al. (2016) noticed WSOC/OC ratio of 0.1, 0.7 and 0.9 for vehicular exhaust, biomass burning and oxidized organic aerosols respectively suggesting OC/WSOC in the study region is mainly contributed by biomass burning. Both concentrations of WSOC and WIOC were increased during winter from that of before (Fig. 3k,l). The mean concentration of OC during March to September ($9.1 \pm 2 \mu\text{g m}^{-3}$) is about 64% lower than that of winter ($14.9 \pm 3 \mu\text{g m}^{-3}$) whereas an insignificant difference in WSOC is observed between former ($4.3 \pm 0.2 \mu\text{g m}^{-3}$) and latter ($4.7 \pm 1 \mu\text{g m}^{-3}$) suggesting that significant modification of OC during transport. The inverse relationship between EC and WIOC during winter suggests that both WOSC and WIOC were modified during their transport to the study region (Fig. 5c). The annual mean WSOC levels over the coastal BoB ($4.5 \pm 0.7 \mu\text{g m}^{-3}$) is within the range reported in the Arabian Sea (2.2-8.6 $\mu\text{g m}^{-3}$; Kumar et al., 2012; Ashwini et al., 2020; Bikkina et al., 2021) and BoB (5.5-6.7 $\mu\text{g m}^{-3}$; Srinivas and Sarin, 2013). The WSOC/WIOC ratio was lower during winter (0.54 ± 0.1) than other months (0.90 ± 0.2) indicating a significant modification of OC during the former period. This study suggests that higher EC was observed during winter compared to other seasons and significant modification of OC was noticed during winter due to long-range transport than other seasons.

To evaluate the contribution of secondary organic carbon (SOC) to total OC, the primary OC/EC ratio was estimated from the source emission using the minimum R-squared (MRS) method (Wu and Yu,

2016). In this method, variable initial primary OC/EC ratios are used to estimate the minimum coefficient of determination of the linear regression between SOC and EC. The estimated primary OC/EC ratio was 3.0 over the study region using the entire data collected (Fig. Supplementary Fig S2). Based on this, SOC is estimated using the following equations:

$$\text{Primary organic carbon (POC)} = (\text{OC/EC})_{\text{primary}} \times \text{EC}$$

$$\text{Secondary organic carbon (SOC)} = \text{OC} - \text{POC}$$

The estimated SOC concentrations varied between 2.7 and 11.9 $\mu\text{g m}^{-3}$ with higher concentrations during winter ($10.9 \pm 1 \mu\text{g m}^{-3}$) than other months ($4.5 \pm 2 \mu\text{g m}^{-3}$) and accounted for 26-65% (av. 50%) of OC and 4-11% (av. 7%) of TSP in the study region. The increased SOC during winter is likely due to low mixing layer height and increased condensable secondary species due to low atmospheric temperature (Gray et al., 1986). Bhowmik et al (2020) noticed that SOC contributed between 36 and 47% to OC in the IGP region whereas it was varied between 30 and 65% in China, Brazil and Mexico (Mancilla et al., 2015; Monteiro dos Santos et al., 2016; Zhang et al., 2012). Several investigators found that SOC is mostly water-soluble as the polar functional groups are formed through oxidation of volatile organic carbon (VOCs), hence WSOC is a reasonable proxy for SOC (Saxena and Hildemann, 1996; Weber et al., 2007).

3.4. Temporal variations in source of aerosols over the BoB

The source of aerosols over the coastal BoB may be contributed by vehicular emissions, coal power plants, biomass burning and fossil fuel burning. To examine the possible dominant sources among them, the mass elemental ratios were used. Since NO_x is emitted from the vehicular emission, which is oxidized to NO_3^- in the atmosphere, it represents fossil fuel burning. The coal burning in the power plants emit SO_2 , which is oxidized to SO_4^{2-} in the atmosphere, and it represents the source from the power plants. The mass ratio of $\text{NO}_3^-/\text{anthropogenic SO}_4^{2-}$ represents the relative importance of these two sources to the atmospheric aerosols (Huebert et al., 1988). This ratio in the TSP is well below unity (0.08 to 0.23: mean of 0.15 ± 0.04) with a relatively higher ratio during May to September (0.2 ± 0.07) than other months (0.1 ± 0.05). These ratios suggest that stationary sources (i.e., from coal burning in power plants) contribute significantly over vehicular emissions to the TSP during the entire study period with a relatively higher contribution of vehicular emission during May to September than other months. The range of $\text{NO}_3^-/\text{anthropogenic SO}_4^{2-}$ ratios reported over the BoB (0.01 to 0.43; Rengarajan et al., 2007) are consistent with the present study.

Aerosols are contributed by biomass burning, coal combustion and mineral dust in the study region. Different diagnostic binary ratios can be used to differentiate sources of aerosols during winter from

that of other seasons as these ratios are significantly different during winter than other months (Supplementary Table T1). The dominant contribution of biomass burning and coal combustion over mineral dust can be assessed using the diagnostic binary ratios of $\text{nss-K}^+/\text{nss-Ca}^{2+}$ and $\text{nss-SO}_4^{2-}/\text{nss-Ca}^{2+}$. Since both nss-K^+ and nss-SO_4^{2-} are produced through biomass burning and coal combustion respectively and nss-Ca^{2+} is a tracer for mineral dust (Rastogi and Sarin, 2006; Srinivas et al., 2014), their ratios will give information on dominant contribution natural versus anthropogenic sources. Both $\text{nss-K}^+/\text{nss-Ca}^{2+}$ and $\text{nss-SO}_4^{2-}/\text{nss-Ca}^{2+}$ mass ratios displayed higher values during winter (5.3 ± 3 and 36.2 ± 26 respectively) than April to October (0.06 ± 0.02 and 3.3 ± 2 respectively; Supplementary Table T1) suggesting that higher contribution of anthropogenic sources (biomass burning and coal combustion) over mineral dust in the former. In contrast, the decrease in $\text{nss-K}^+/\text{nss-Ca}^{2+}$ and $\text{nss-SO}_4^{2-}/\text{nss-Ca}^{2+}$ mass ratios during April to October indicates an increase in the relative contribution of mineral dust than winter. The air-mass back trajectories suggest that air masses were originated from the IGP region during winter resulting in a higher contribution of biomass burning whereas local processes are important during other months as air mass is travelled from central or southern India (Fig. 1).

In addition to this, OC/EC , $\text{nss-K}^+/\text{EC}$, $\text{nss-K}^+/\text{OC}$ and $\text{nss-SO}_4^{2-}/\text{EC}$ ratios can also be used to evaluate relative sources from biomass burning and coal combustion. The OC/EC mass ratio varies between 2 and 4 for fossil fuel combustion whereas 4 to 12 in the case of biomass burning. The OC/EC ratios over the coastal BoB was 8.8 ± 1.6 during winter and 5.8 ± 0.8 during March to October period (Fig 6d; Supplementary Table T1) indicating that the dominant contribution of biomass burning emissions in the study region during the former period and the contribution from fossil fuel is relatively higher during the latter period. This interpretation is further confirmed by $\text{nss-K}^+/\text{EC}$ mass ratios (0.4 ± 0.1 during winter and 0.05 ± 0.01 during other months) (Fig. 6e) and $\text{nss-K}^+/\text{OC}$ (0.06 ± 0.01 during winter and 0.01 ± 0.01 during other months; Supplementary Table T1) (Fig. 6f) and the ratios observed during winter are close to that burning of crop-residues in the IGP during (0.79 ± 0.22) and other months (0.07 ± 0.04 ; Srinivas and Sarin, 2014) suggesting that dominant contribution of biomass burning to the carbonaceous aerosol over the coastal BoB during winter and its contribution to TSP decreased during March to October due to reversing the direction of winds (Fig. 1).

The NSS-SO_4^{2-} can be used to trace the influence of anthropogenic sources from continental sources as it exhibits a similar trend of EC. During winter, the study region is influenced by the continental outflow from the IGP region as evidenced by a higher concentration of nss-SO_4^{2-} ($34.6 \mu\text{g m}^{-3}$) in the TSP compared to other periods ($13.5 \mu\text{g m}^{-3}$). A significant linear relationship was observed between

EC and nss-SO_4^{2-} ($r^2=0.32$; $p<0.001$) in the coastal BoB suggesting continental source is a significant source. To further evaluate the contribution of SO_4^{2-} from coal combustion and vehicular emissions, $\text{nss-SO}_4^{2-}/\text{EC}$ ratios were used (Supplementary Table T1; Fig. 6g). National Thermal Powerplant Corporation (NTPC; <https://www.ntpc.co.in>) is located ~30 km away from the study region, which is one of the main sources of ambient SO_2 and EC. In contrast, a high amount of EC is emitted to the atmosphere through both vehicular emissions and biomass burning whereas the emission of SO_2 is low. Since SO_2 in the atmosphere has a short lifetime (<2 h to 2 days; Pandis and Seinfeld, 2006; Mallik et al., 2013), it converts rapidly to SO_4^{2-} . Hence, $\text{SO}_4^{2-}/\text{EC}$ mass ratio acts as a pseudo-tracer for the continental outflows. The $\text{nss-SO}_4^{2-}/\text{EC}$ ratio varies between 1.4 and 2.8 due to biomass burning (Kundu et al., 2010; Rajput et al., 2014b; Rastogi et al., 2015), 3.9 ± 2.1 in the coal-fired power plant, and 6.2 ± 3.6 in the IGP-outflow to the BoB (Srinivas and Sarin, 2012) and the Arabian Sea (Bikkina et al., 2020). The $\text{nss-SO}_4^{2-}/\text{EC}$ ratio from the BoB (16.7 ± 4 and 8.7 ± 3 during winter and other months respectively; Fig. 6g; Supplementary Table T1) suggests that SO_4^{2-} is sourced mainly from coal combustion over the coastal BoB.

The major contributors of organic carbon to the atmosphere come from the emission of fossil-fuel combustion and biomass burning. The relative importance of these sources can be evaluated based on WSOC/OC ratio in the TSP as WSOC contribution due to fossil fuel combustion is lower (Aggarwal et al., 2013) than biomass burning. Hence, a higher WSOC/OC ratio (0.65 ± 0.14 ; Kundu et al., 2010) denotes a significant contribution from biomass burning and vice versa for fossil fuel combustion. Bikkina et al. (2020) reported a WSOC/OC ratio of 0.59 ± 0.2 over the MABL of the Arabian Sea and it is close to emissions from biomass burning in the IGP (0.52 ± 0.16 ; Srinivas and Sarin, 2014; Rajput et al., 2014). The mean ratio of WSOC/OC was 0.42 ± 0.1 in the coastal BoB, which is close to that of the values reported in the Arabian Sea and IGP region (Bhowmik et al., 2020) suggesting that a significant fraction of biomass burning may be contributing to the OC. The lower ratio of WSOC/OC may be caused by modification of WSOC during transport from the source region. The WIOC and EC displayed a linear relationship during all seasons except winter when inverse relation was observed (Fig. 5d). The mean ratio of WIOC/EC was 3.3 ± 0.6 from March to October whereas it was slightly higher (3.9 ± 2) during winter in the study region (Supplementary Table T1). The WIOC/EC ratios in the study region are close to that reported in the IGP outflow region (3.7 ± 1.5 ; Srinivas and Sarin, 2014) suggesting a significant contribution of aerosols from the IGP region.

Kim et al. (2015) suggested that wind direction and speed significantly influences the transport of particle-bound compounds in the atmosphere. Grundstrom et al. (2015) also reported the influence of

atmospheric circulation on air quality in the urban region. Since the direction of wind reverses between winter and summer due to northeast and southwest monsoon respectively, the sources of aerosols and elemental ratios may be varied significantly with reference to the direction of the wind. To examine the same, the diagnostic mass ratios, such as OC/EC, $\text{NO}_3^-/\text{SO}_4^{2-}$, $\text{nss-SO}_4^{2-}/\text{EC}$, $\text{NH}_4^+/\text{SO}_4^{2-}$, WIOC/EC, $\text{nss-SO}_4^{2-}/\text{nss-Ca}^{2+}$ and $\text{nss-K}^+/\text{nss-Ca}^{2+}$, data have been divided with reference to the direction of the wind (8 groups-N, NE, E, SE, S, SW, W, and NW). During the entire study period wind-blown from all directions, except east (E) and southwestern (SW) direction. Therefore, data from the 6 groups were subjected to an ANOVA test. The ANOVA results indicated significant differences ($p < 0.01$) between groups for the elemental ratios mentioned above suggesting the direction of the wind has a significant impact on the elemental ratios in the aerosols. The post-hoc test suggested that OC/EC, $\text{NO}_3^-/\text{SO}_4^{2-}$, $\text{nss-SO}_4^{2-}/\text{EC}$, $\text{NH}_4^+/\text{SO}_4^{2-}$, WIOC/EC, $\text{nss-SO}_4^{2-}/\text{nss-Ca}^{2+}$ and $\text{nss-K}^+/\text{nss-Ca}^{2+}$ were significant different ($p < 0.01$) between the aerosols come from western/ southern and north/northwestern directions. The western or southern winds bring aerosols from central or south India whereas aerosols from IGP are brought to the study region by northern and northwestern winds. The central and south Indian aerosols are dominantly contributed by vehicular emissions (Kommula et al., 2021; Ramachandran, 2005) whereas the IGP region is mainly contributed by biomass burning, hence, the elemental ratios are significantly different.

3.5. Nature of aerosols

Sarma et al. (2015) found that rapid acidification of surface waters in the northwestern coastal BoB due to deposition of aerosols during spring intermonsoon. Yadav et al. (2019) found aerosols over the coastal BoB were acidic during the winter and spring monsoon periods. Recently Kumari et al. (2021) found that aerosols throughout the year were acidic however the strength of the acidity is higher during winter and the least during summer. To examine the acidity of the aerosols over the coastal BoB, the equivalent mass ratios of NH_4^+ to nss-SO_4^{2-} in the TSP were examined. This ratio was lower than unity during the entire year (0.02-0.87 mean of 0.38 ± 0.2) (Fig. 6i) indicating that excess non-sea salt SO_4^{2-} over NH_4^+ suggests the presence of acidic nature of aerosols over the BoB. The mean ratio of $\text{NH}_4^+/\text{nss-SO}_4^{2-}$ of ~ 0.7 was reported over the Arabian Sea during winter (Kumar et al., 2012; Ashwini et al., 2020; Bikkina et al., 2021) suggesting aerosols over the Arabian Sea were relatively less acidic than BoB.

Nature (acidic versus basic) of aerosols can be understood from the balance between equivalent cations and anions. Excess anions over the cations result in acidic nature and vice versa represents basic nature (Han et al. 2007). The computed ratio of neutralization potential to acidic potential (NP/AP), based on equations 1 and 2 in section 2.4, was less than unity with a mean value of 0.80 ± 0.1 , except March

and May, suggesting that aerosols over the coastal BoB are acidic in nature (Fig. 7a). Similarly, the total hydrogen ions ($[H^+]_T$) were ranged between 0.23 and 0.99 with a mean of $0.64 \pm 0.2 \mu\text{eq m}^{-3}$ in the study region (Fig. 7b) further confirming that the acidic nature of aerosols in the study region with higher concentration during October to February than other periods suggesting aerosols are highly acidic during winter than other periods. The acidic nature of aerosols was reported in the coastal BoB during 2013 and 2015 as well (Yadav et al., 2019; Kumari et al., 2021).

Bikkina et al. (2020) found that aqueous phase chemical reactions do not influence significantly the formation of WSOC over the Arabian Sea and it is attributed to the alkaline nature of TSP over the Arabian Sea due to the dominant influence of dust. In contrast, the abundance of WSOC over the BoB is controlled by aerosol acidity during the winter season (Srinivas et al., 2017). We noticed an inverse correlation of WSOC with ambient air temperature and relative humidity over the coastal BoB (Supplementary Fig. S3a,b) suggesting that the formation of secondary organic aerosols (SOA) is possible at higher moisture and temperature conditions. Srinivas et al. (2017) reported the occurrence of SOAs, such as oxalic acid, succinic acid and glyoxylic acids, in the outflow of IGP and attributed to their production in the aqueous phase through photochemical reactions, which were largely controlled by anthropogenic SO_4^{2-} . Therefore, the acidity of the aerosols may be further contributed by organic acids, in addition to, the dominance of anions over the cations resulting in rapid acidification of coastal BoB. Kumari et al. (2021) found that the lowering of pH due to the addition of aerosols into the surface water displayed a significant relationship with NO_3^- and SO_4^{2-} in the aerosols. Recently Sarma et al. (2021) reported that coastal BoB is acidifying rapidly, by three times than elsewhere in the world in the low-latitude regions due to the deposition of atmospheric pollutants. Since SO_4^{2-} contributes to ~50% of the water-soluble inorganic species (WSIS) in the TSP, the source of SO_4^{2-} is needed to identify to understand the rapid acidification of coastal waters.

3.6. Contribution of various sources of SO_4^{2-} in the TSP

SO_4^{2-} in the TSP is contributed by both anthropogenic and biogenic sources. The dimethyl sulphide (DMS) is, produced by several phytoplankton due to stress caused by nutrients and salinity (Shenoy and Patil, 2003), released to the atmosphere, where it gets oxidized to Methanesulfonic acid (MSA). Both DMS and its oxidative products are considered to be a source of nss- SO_4^{2-} (Hatakeyama and Akimoto, 1983; Hatakeyama et al., 1985). Viswanadham et al. (2015) reported higher concentrations of DMSP and DMS in the coastal BoB due to severe stress caused by salinity stratification and low nutrient levels. This resulted in the estimated flux of DMS to the atmosphere of $5.5 \pm 4 \mu\text{mol S m}^{-2} \text{d}^{-1}$ to the atmosphere. Therefore, the significant contribution of biogenic SO_4^{2-} is possible over the BoB.

Johansen et al. (1999) found a significant contribution of biogenic and anthropogenic sources to the nss-SO₄²⁻ in the Arabian Sea. The biogenic SO₄²⁻ can be estimated following Bikkina et al. (2020)

$$\text{Biogenic SO}_4^{2-} = [\text{MSA}]_{\text{aerosol}} \times (\text{nss-SO}_4^{2-}/\text{MSA})_{\text{bio}}$$

Where [MSA]_{aero} is the concentration of MSA in the TSP and the ratio of nss-SO₄²⁻ to MSA is represented by (nss-SO₄²⁻/MSA)_{bio} and this ratio is mainly influenced by biological activity. This ratio of 0.05-0.06 was proposed based on the significant linear relationship between nss-SO₄²⁻ and MSA in the tropical marine aerosols (Savoie and Prospero, 1989) whereas Johansen and Hoffman (2004) proposed a relationship between temperature and nss-SO₄²⁻/MSA ratio. Recently Bikkina et al. (2020) measured MSA over the coastal Arabian Sea and found that the MSA/nss-SO₄²⁻ ratio of 0.007±0.004 and is close to that of the same estimated (0.0068) based on Johansen and Hoffman (2004) model at a mean temperature of 28.7°C. Based on this relationship, MSA in the TSP over the coastal BoB was computed and it was varied between 0.06 and 0.29 µg m⁻³ (mean 0.1±0.06 µg m⁻³) (Fig. 8a). The estimated biogenic SO₄²⁻ varied between 0.9 and 4.46 µg m⁻³ (mean of 2.19±0.9 µg m⁻³) with higher concentrations during winter (3.36±1 µg m⁻³) than other months (1.45±0.4 µg m⁻³) (Supplementary Fig. S3b). The anthropogenic SO₄²⁻ varied between 7.6 to 38.0 mg m⁻³ with higher concentrations during October to February (31.2±8 µg m⁻³) than other months (12.4±2 µg m⁻³) (Supplementary Fig. S3c). The mean contribution of biogenic SO₄²⁻ to total SO₄²⁻ during the entire study period was ~10±0.7% (Supplementary Fig. S3d) suggesting that anthropogenic contribution is a very significant source of nss-SO₄²⁻ in the coastal BoB. Bikkina et al. (2020) reported that the contribution of biogenic SO₄²⁻ to total SO₄²⁻ was varied between 2.3 and 22% (mean of 17±6%) and it is consistent with the DMS concentrations and fluxes to the atmosphere (Shenoy and Kumar, 2007). They noticed that the concentration of DMS is almost more than three times higher in the Arabian Sea than BoB due to the high primary production and higher abundance of phytoplankton that produces DMS. Despite higher concentrations of DMS in the Arabian Sea, the flux is higher in the BoB due to higher wind speed, which shows significant interannual variability. Therefore, the contribution of DMS to total SO₄²⁻ in the aerosols were less in the BoB than in the Arabian Sea. It is further confirmed that the higher acidity of the aerosols over the BoB is significantly contributed by the SO₄²⁻ emitted by the coal combustion that resulted in rapid acidification of the surface waters of the coastal BoB.

5. Summary and Conclusions

The ionic and carbonaceous components displayed significant temporal variability over the coastal Bay of Bengal (BoB) due to reversing the direction of winds due to monsoons. The air mass back trajectories suggested that the aerosols were brought from the IGP region during October to February

whereas central and southern Indian peninsula during other months. The higher TSP concentrations were observed during winter suggests IGP contributed higher aerosols over the study region than peninsular India. Sulphate contributed more >40% of water-soluble inorganic species (WSIS) followed by sodium, ammonium and nitrate. The contribution of anthropogenic SO_4^{2-} is the highest (>70%) followed by sea salt and biogenic sources. Based on ionic ratios, coal burning is the dominant source of aerosols from March to September whereas biomass burning contributed significantly during October to February over the coastal BoB. The charge balance of ionic composition suggests the acidic nature of aerosols. This study has implications for understanding the evolving nature of secondary inorganic and organic aerosols in the continental outflows and potential sources responsible for the acidification of coastal waters. This study further suggested that atmospheric aerosols are acidic in nature and acidify coastal waters and their impact on the ecosystem needs further evaluation.

Acknowledgements: The senior author (VRK) would like to thank the Department of Science and Technology for the fellowship. We would like to Director, CSIR-National Institute of Oceanography for encouragement and support. We like to thank the NOAA Air Resources Laboratory for the access to the HYSPLIT model. We appreciate for making available MODIS aerosol optical depth data by NASA Goddard Earth Sciences Data and Information Services Center. We would like to thank two anonymous reviewers for their critical review to improve the presentation of our results. This has the NIO contribution number.....

References

- Aggarwal, S.G., Kawamura, K., Umarji, G.S., Tachibana, E., Patil, R.S., Gupta, P.K., 2013. Organic and inorganic markers and stable C-, N-isotopic compositions of tropical coastal aerosols from megacity Mumbai: sources of organic aerosols and atmospheric processing. *Atmos. Chem. Phys.* 13, 4667–4680. <https://doi.org/10.5194/acp-13-4667-2013>.
- Andrae, M.O., Ramanathan, V., 2013. Climate's dark forcings. *Science*. 340, 280-281. <https://doi.org/10.1126/science.1235731>.
- Ashwini, A.R., Hegde, P., Aryasree, S., Girach, I.A., Nair, P.R., 2020. The continental outflow of anthropogenic aerosols over Arabian Sea and Indian Ocean during wintertime: ICARB-2018 campaign. *Sci. Total Environ.* 712, 135214. <https://doi.org/10.1016/j.scitotenv.2019.135214>.
- Bhowmik, H.S., Naresh, S., Bhattu, D., Rastogi, N., Prevot, A.S.H., and Tripathi, S.N., 2021. Temporal and spatial variability of carbonaceous species (EC; OC; WSOC and SOA) in PM_{2.5} aerosol over five sites of Indo-Gangetic Plain. *Atm. Poll. Res.* 12, 375-390. <https://doi.org/10.1016/j.apr.2020.09.019>.
- Bikkina, P., Sarma, V.V.S.S. Kimitaka Kawamura, Srinivas, B., Bhagawati, K., Sherin, C.K., 2020. Chemical characterization of wintertime aerosols over the Arabian Sea: Impact of marine sources and long-range transport. *Atmos. Environ.* 239, 117749. <https://doi.org/10.1016/j.atmosenv.2020.117749>.
- Bikkina, P., Sarma, V.V.S.S., Kimitaka Kawamura., Srinivas, B., 2021. Dry-deposition of inorganic and organic nitrogen aerosols to the Arabian Sea: Sources, transport and biogeochemical significance in surface waters. *Mar. Chem.* 231, 103938. <https://doi.org/10.1016/j.marchem.2021.103938>.
- Birch, M.E., Cary, R.A., 1996. Elemental Carbon-Based Method for Monitoring Occupational Exposures to Particulate Diesel Exhaust. *Aerosol Sci. Technol.* 25, 221–241. <https://doi.org/10.1080/02786829608965393>.
- Bond, T.C., Bergstorm, R.W., 2006. Light absorption by carbonaceous particles: an investigative review. *Aerosol. Sci. Technol.* 40, 27-67. <https://doi.org/10.1080/02786820500421521>.
- Chen, P., Kang, S., Li, C., Zhang, Q., Guo, J., Tripathee, L., Zhang, Y., Li, G., Gul, C., Cong, Z., Wan, X., Niu, H., Panday, A.K., Rupakheti, M., Ji, Z., 2019. Carbonaceous aerosol characteristics on the Third Pole: a primary study based on the Atmospheric Pollution and Cryospheric Change (APCC) network. *Environ. Pollut.* 253, 49-60. <https://doi.org/10.1016/j.envpol.2019.06.112>.
- Cheung, K.L., Polidori, A., Ntziachristos, L., Tzamkiozis, T., Samaras, Z., Cassee, F.R., Gerlofs, M., Sioutas, C., 2009. Chemical characteristics and oxidative potential of particulate matter emissions from gasoline, diesel, and biodiesel cars. *Environ. Sci. Technol.* 43 (16), 6334-6340. <https://doi.org/10.1021/es900819t>.
- ChooChuay, C., Pongpiachan, S., Tipmanee, D., Suttinun, O., Deelaman, W., Wang, Q., Xing, L., Li, G., Han, Y., Palakun, J., Cao, J. 2020. Impacts of PM_{2.5} sources on variations in particulate chemical compounds in ambient air of Bangkok, Thailand. *Atmos. Pollu. Res.* 11 (9), 1657-1667. <https://doi.org/10.1016/j.apr.2020.06.030>.

Cooke, W.F., Lioussé, C., Cachier, H., Feichter, J., 1999. Construction of a $1^\circ \times 1^\circ$ degree fossil fuel emission data set for carbonaceous aerosol and implementation and radiative impact in the ECHAM4 model. *J. Geophys. Res.* 104, 22,137-22,162. <https://dx.doi.org/10.1029/1999JD900187>.

Cruz, M.T., Banage, P.A., Betito, G., Braun, R.A., Stahl, C., Aghdam, M.A., Cambaliza, M. O., Dadashazar, H., Hilario, M.R., Lorenzo, G.R., Ma, L., MacDonald, A.B., Pabroa, P. C., Yee, J.R., Simpas, J.B., Sorooshian, A., 2019. Size-resolved composition and morphology of particulate matter during the southwest monsoon in Metro Manila, Philippines. *Atmos. Chem. Phys.* 19, 10675–10696. <https://doi.org/10.5194/acp-19-10675-2019>, 2019.

Daellenbach, K.R., Bozzetti, C., Krepelova, A., Canonaco, F., Wolf, R., Zotter, P., Fermo, P., Crippa, M., Slowik, J.G., Sosedova, Y., Zhang, Y., Huang, R.J., Poulain, L., Szidat, S., Baltensperger, U.I., Haddad, El., Prevot, A.S.H., 2016. Characterization and source apportionment of organic aerosol using offline aerosol mass spectrometry. *Atmos. Meas. Tech.* 9 (1), 23-39. <https://doi:10.5194/amt-9-23-2016>, 2016.

Decesari, S., Fuzzi, S., Facchini, M.C., Mircea, M., EmblicomL., Cavalli, F., Maenhaut, W., Chi, X., Schkolnik, G., Falkovich, A., Rudich, Y., Claeys, M., Pashynska, V., Vas, G., Kourtchev, I., Vermeylen, R., Hoffer, A., Andreae, M.O., Tagliavini, E., Moretti, F., and Artaxo, P., 2006. Characterization of the organic composition of aerosols from Rondonia, Brazil, during the LBA-SMOCC 2002 experiment and its representation through model compounds. *Atmospheric Chem. Phys.* 6, 375-402. <https://doi.org/10.5194/acp-6-375-2006>.

Doney, S. C., Mahowald, N., Lima, I., Feely, R. A., Mackenzie, F. T., Lamarque, J.F., Rasch, P.J., 2007. Impact of anthropogenic atmospheric nitrogen and sulfur deposition on ocean acidification and the inorganic carbon system. *Proc. Natl. Acad. Sci.* 104, 14580-14585. <https://doi.org/10.1073/pnas.0702218104>.

Draxler, R.R., 1999. HYSPLIT4 user's guide. NOAA Tech. Memo. ERL ARL-230, NOAA Air Resources Laboratory, Silver Spring, MD.

Draxler, R., Rolph, G., 2009. HYSPLIT (Hybrid Single-Particle Lagrangian Integrated Trajectory) Model access via NOAA ARL READY Website. NOAA Air Resources Laboratory, Silver Spring, MD, 2003.

Fadnavis, S., Rolf Muller., Gayatri Kalita., Matthew Rowlinson., Alexandru Rap., Jui-Lin Frank Li., Blaz Gasparini., Anton Laakso., 2019. The impact of recent changes in Asian anthropogenic emissions of SO₂ on sulfate loading in the upper troposphere and lower stratosphere and the associated radiative changes. *Atmos. Chem. Phys.* 19, 9989–10008. <https://doi.org/10.5194/acp-19-9989-2019>.

Favez, O., Sciare, J., Cachier, H., Alfaro, S.C., Abdelwahab, M.M., 2008. Significant formation of water-insoluble secondary organic aerosols in a semi-arid urban environment. *Geophys. Res. Lett.* 35. <https://doi.org/10.1029/2008GL034446>.

Flores, R.M., Ozdemir, H., Akkoyunlu, B.O., Unal, ALper, Tayanc, M., 2020. Seasonal variation of carbonaceous PM_{2.5} in an Istanbul traffic site. *Atm. Poll. Res.* 11, 2110-2118. <https://doi.org/10.1016/j.apr.2020.06.022>.

Gray, H.A., Cass, G.R., Huntzicker, J.J., Heyerdahl, E.K., Rau, J.A., 1986. Characteristics of atmospheric organic and elemental carbon particle concentrations in Los Angeles. *Environ. Sci. Technol.* 20 (6), 580-589 <https://doi.org/10.1021/es00148a006>.

Gogoi, M.M., Babu, S.S., Moorthy, K.K., Bhuyan, P.K., Pathak, B., Subha, I., Chutia, L., Kundu, S.S., Bharali, C., Borgohain, A., Guha, A., De, B.K., Singh, B., Chin, M., 2017. Radiative effects of absorbing aerosols over northeastern India: observations and model simulations. *J. Geophys. Res: Atmospheres.* 122, 1132-1137. . <https://doi.org/10.1002/2016JD025592>.

Grundstrom, M., Tang, L., Hallquist, M., Nguyen, H., Chen, D., Pleijel, H., 2015. Influence of atmospheric circulation patterns on urban air quality during the winter. *Atm. Poll. Res.* 6, 278-285. <https://doi.10.5094/APR.2015.032>.

Gundel, L.A., Guyot-Sionnest, N.S., Novakov, T., 1989. A study of the interaction of NO₂ with carbon particles. *Aerosol Sci. Tech.* 10, 343-351. <https://doi.org/10.1080/02786828908959271>.

Han, L., Zhuang, G., Cheng, S., Li, J., 2007. The Mineral Aerosol and Its Impact on Urban Pollution Aerosols over Beijing, China. *Atmos. Environ.* 41, 7533–7546. <https://doi:10.1016/j.atmosenv.2007.05.046>.

Hatakeyama, S., Akimoto, H., 1983. Reactions of hydroxyl radicals with methanethiol, dimethyl sulfide, and dimethyl disulfide in air. *J. Phys. Chem.* 87, 2387–2395. <https://doi.org/10.1021/j100236a029>.

Hatakeyama, S., Izumi, K., Akimoto, H., 1985. Yield of SO₂ and formation of aerosol in the photo-oxidation of DMS under atmospheric conditions. *Atmos. Environ.* 19(19), 135–141. [https://doi.org/10.1016/0004-6981\(85\)90144-1](https://doi.org/10.1016/0004-6981(85)90144-1).

Hu, Z.F., Kang, S.C., Li, C.L., Yan, F.P., Chen, P.F., Gao, S.P., Wang, Z.Y., Zhang, Y.L., Sillanpa, M., 2017. Light absorption of biomass burning and vehicle emission- sourced carbonaceous aerosols of the Tibetan Plateau. *Environ. Sci. Pollut. Res.* 24, 15369-15378. <https://doi.10.1007/s11356-017-9077-3>.

Huebert, B.J., Ming-Xing, W., Wei-Xiu, L., 1988. Atmospheric nitrate, sulfate, ammonium and calcium concentrations in China. *Tellus B.* 40B, 260–269. <https://doi.org/10.3402/tellusb.v40i4.15914>.

Jafar, H.A., Harrison, R.M., 2020. Spatial and temporal trends in carbonaceous aerosols in the United Kingdom. *Atmos. Poll. Res.* 12 (1), 295-305. <https://doi.org/10.1016/j.apr.2020.09.009>.

Ji, Z.M., Kang, S.C., Zhang, D.F., Zhu, C.Z., Wu, J., XU., 2011. Simulation of anthropogenic aerosols over South Asia and their effects on Indian summer monsoon. *Clim Dyn.* 36, 1633-1647. <https://doi.org/10.1007/s00382-015-2509-1>.

Ji, D., Gao, M., Maenhaut, W., He, J., Wu, C., Cheng, L., Gao, W., Sun, Y., Sun, J., Xin, J., Wang, L., Wang, Y., 2019. The carbonaceous aerosol levels still remain a challenge in the Beijing-Tianjin-Hebei region of China: insights from continuous high temporal resolution measurements in multiple cities. *Environ. Int.* 126 (February), 171-183. <https://doi.org/10.1016/j.envint.2019.02.034>.

Jickells, T.D., et al., 2005. Global iron connections between desert dust, ocean biogeochemistry and climate. *Science*. 308, 67e71. <https://doi:10.1126/science.1105959>.

Johansen, A.M., Hoffmann, M.R., 2004. Chemical characterization of ambient aerosol collected during the northeast monsoon season over the Arabian Sea: anions and cations. *J. Geophys. Res.: Atmospheres*. 109, D05305. <https://doi:10.1029/2003JD004111>.

Johansen, A.M., Siefert, R.L., Hoffmann, M.R., 1999. Chemical characterization of ambient aerosol collected during the southwest monsoon and intermonsoon seasons over the Arabian Sea: anions and cations. *J. Geophys. Res.: Atmospheres*. 104, 26325–26347. <https://doi:10.1029/1999JD900405>.

Jose, J., Srimuruganandam, B., Nagendra, S.M.S., 2019. Characterization of PM10 and PM2.5 emission sources at Chennai, India. *Nat. Env. And Poll. Tech.* 18, 555-562.

Keene, W.C., Pszenny, A.A., Galloway, J.N., Hawley, M.E., 1986. Sea-salt corrections and interpretation of constituent ratios in marine precipitation. *J. Geophys. Res.: Atmospheres*. 1984–2012 (91), 6647–6658. <https://doi.org/10.1029/JD091iD06p06647>.

Khemani, L. T., Momin, G. A., Naik, M. S., Rao, P. S. P., Kumar, R. and Murty, Ramana Bh. V., 1985. Trace elements and sea salt aerosols over the sea areas around the Indian sub-continent. *Atmos. Environ.* 19, 277-284. [https://doi-10.1016/0004-6981\(85\)90095-2](https://doi-10.1016/0004-6981(85)90095-2).

Kim, K.H., Lee, S.B., Woo, D., Bae, G.N., 2015. Influence of wind direction and speed on the transport of particle-bound PAHs in a roadway environment. *Atm. Poll. Res.* 6, 1024-1034. <https://doi.org/10.1016/j.apr.2015.05.007>.

Kommula, S.M., Upasana, P., Sharma, A., Raj, S.S., Reyes-villegas, E., Liu, T., Allan, J.D., Jose, C., Pohlker, M., Ravikrishna, R., Liu, P., Su, H., martin, S.T., Poschl, U., Mcfiggans, G., Coe, H., and Gunthe, S.S. 2021. Chemical characterization and Source apportionment of organic aerosols in the coastal city of Chennai, India: Impact of marine air masses on aerosol chemical composition and potential for secondary organic aerosol formation. *ACS Earth Space Chem.* 5,11, 3197-3209. <https://doi:10.1021/acsearthspacechem.1c00276>.

Kulshrestha, U.C., Saxena, A., Kumar, N., Kumari, K.M., Srivastava, S.S., 1998. Chemical composition and Association of Size-Differentiated Aerosols at a Suburban Site in a Semi-Arid Tract of India. *Jl. Atmos. Chem.* 29, 109-118. <https://doi.org/10.1023/A:1005796400044>.

Kumar, A., Sarin, M.M., Sudheer, A.K., 2008a. Mineral and anthropogenic aerosols in Arabian Sea–atmospheric boundary layer: sources and spatial variability. *Atmos. Environ.* 42, 5169–5181. <https://doi:10.1016/j.atmosenv.2008.03.004>

Kumar, A., Sudheer, A, Sarin, M., 2008b. Chemical characteristics of aerosols in MABL of Bay of Bengal and Arabian Sea during spring inter-monsoon a comparative study. *J. Earth Syst. Sci.* 117, 325-332. <https://doi:10.1007/s12040-008-0035-9>.

Kumar, A., Sudheer, A.K., Goswami, V., Bhushan, R., 2012. Influence of continental outflow on aerosol chemical characteristics over the Arabian Sea during winter. *Atmos. Environ.* 50, 182-191. <https://doi:10.1016/j.atmosenv.2011.12.040>.

- Kumari, V. R., Yadav, K., Sarma, V.V.S.S., Kumar, M. D., 2021. Acidification of the coastal Bay of Bengal by aerosol deposition. *J. Earth Sys. Sci.* 130: 223. <https://doi: 10.1007/s12040-021-01723-x>.
- Kundu, S., Kawamura, K., Andreae, T.W., Hoffer, A., Andreae, M.O., 2010. Diurnal variation in the water-soluble inorganic ions, organic carbon and isotopic compositions of total carbon and nitrogen in biomass burning aerosols from the LBA- SMOCC campaign in Rondonia, Brazil. *J. Aerosol Sci.* 41, 118–133. <https://doi.org/10.1016/j.jaerosci.2009.08.006>.
- Kurokawa, J., Ohara, T., 2020. Long-term historical trends in air pollutant emissions in Asia: Regional Emission inventory in Asia (REAS) version 3. *Atmos. Chem. Phys.* 20, 12761–12793. <https://doi.org/10.5194/acp-20-12761-2020>.
- Lee, C., Martin, R.V., van Donkelaar, A., Lee, H., Dickerson, R.R., Hains, J.C., Krotkov, N., Richter, A., Vinnikov, K., Schwab, J.J., 2011. SO₂ emissions and lifetimes: estimates from inverse modeling using in situ and global, space-based (SCIAMACHY and OMI) observations. *J. Geophys. Res.: Atmospheres.* 116. D06304. <https://doi:10.1029/2010JD014758>, 2011.
- Lim, H. J., Turpin, B. J., Russell, L. M., and Bates, T. S., 2003. Organic and Elemental Carbon Measurements during ACE-Asia Suggest a Longer Atmospheric Lifetime for Elemental Carbon, *Environ. Sci. Technol.* 37, 3055–3061. <https://doi:10.1021/es020988s>, 2003.
- Ma, Q., Chen, Y., Wang, F., Li, Haowen. 2021. Responses of primary productivity and phytoplankton community to the atmospheric nutrient deposition in the East China Sea. *Atmosphere.* 12, 210. <https://doi.org/10.3390/atmos.12020210>.
- Mahadevan, T. N., Negi, B. S., Meenakshy, V., 1989. Measurements of elemental composition of aerosol matter and precipitation from a remote background site in India. *Atmos. Environ.* 23, 869- 874. [https://doi. 10.1016/0004-6981\(89\)90493-9](https://doi. 10.1016/0004-6981(89)90493-9).
- Mahowald, N., Kloster, S., Engelstaedter, S., Moore, J.K., Mukhopadhyay, S., Albani S. McConnell., Doney, S., Bhattacharya, A., Curran, M., Flanner, M., M., Hoffman, F., Lawrence, D., Lindsay, K., Mayewski, P., Neff, J., Rothenberg, D., Thomas, E., Thornton, P., Zender, C., , C., 2010. Observed 20th century desert dust variability: impact on climate and biogeochemistry. *Atmos. Chem. Phys.* 10, 10875-10893. <https://doi:10.5194/acp-10-10875-2010>.
- Mallik, C., Lal, S., Naja, M., Chand, D., Venkataramani, S., Joshi, H., Pant, P., 2013. Enhanced SO₂ concentrations observed over northern India: role of long-range transport. *Int. J. Rem. Sens.* 34, 2749–2762. <https://doi:10.1080/01431161.2012.750773>.
- Mancilla, Y., Herckes, P., Fraser, M.P., Mendoza, A., 2015. Secondary organic aerosol contributions to PM_{2.5} in Monterrey, Mexico: temporal and seasonal variations. *Atmos. Res.* 153, 348-359. <https://doi.org/10.1016/j.atmosres.2014.09.009>.
- Maranen, E., Fernandez, A., Mourino-Carballido, B., Martinex-Garcia, S., Teira, E., Cermeno, P., Choucino, P., Huete-Ortega, M., Fernandez, E., Calvo-Diaz, A. et al., 2010. Degree of oligotrophy controls the response of microbial plankton to Saharan dust. *Limnol. Oceanogr.* 55, 2339-2352. <https://doi:10.4319/lo.2010.55.6.2339>.

- Martins Pereira, G., Teinla, K., Custodio, D., Gomes Santos, A., Xian, H., Hilamo, R., Alves, C.A., Bittencourt De Andrade, J., Olimpio Da Rocha, G., Kumar, P., Balasubramanian, R., De Fatima Andrade, M., Vasconcellos, P.D.C., 2017. Particulate pollutants in the Brazilian city of Sao Paulo: 1-year investigation for the chemical composition and source apportionment. *Atmos. Chem. Phys.* 17, 11943-11969. <https://doi.org/10.5194/acp-17-11943-2017>.
- Momin G.A., Rao P.S.P., Safai P.D., Ali K., Naik M.S. and Pillai A.G., 1999. Atmospheric aerosol characteristic studies at Pune and Thiruvananthapuram during INDOEX programme-1998. *Current Sci.* 76, 985-989. <http://www.jstor.org/stable/24101378>.
- Monteiro dos Santos, D.A., Brito, J.F., Godoy, J.M., Artaxo, P., 2016. Ambient concentrations and insights on organic and elemental carbon dynamics in Sao Paulo, Brazil. *Atmos. Environ.* 144, 226-233. <https://doi/10.1016/j.atmosenv.2016.08.081>.
- Niranjan, K., Madhavan, B., Sreekanth, V., 2007. Micro Pulse LIDAR observation of high altitude aerosol layers at Visakhapatnam located on the east coast of India. *Geophys. Res. Lett.* 34, L03815. <https://doi:10.1029/2006GL028199>.
- Niranjan, K., Spandana, B., Anjana Devi, T., Sreekanth, V., Madhavan, B.L., 2011. Measurements of aerosol intensive properties over Visakhapatnam, India for 2007. *Ann. Geophys.* 29, 973–985. <https://doi:10.5194/angeo-29-973-2011>.
- Pandis, S.N., Seinfeld, J.H., 2006. *Atmospheric Chemistry and Physics: from Air Pollution to Climate Change*. Wiley.
- Pio, C.A., Legrand, M., Oliveira, T., Afonso, J., Santos, C., Caseiro, A., Fialho, P., Barata, F., Puxbaum, H., Sanchez-Ochoa, A., Kasper-Giebl, A., Gelencser, A., Preunkert, A., and Schock, M., 2007. Climatology of aerosol composition (organic versus inorganic) at nonurban sites on a west-east transect across Europe. *J. Geophys. Res. Atmospheres.* 112, (D23). <https://doi.org/10.1029/2006JD008038>.
- Rajput, P., Sarin, M., Sharma, D., Singh, D., 2014a. Characteristics and emission budget of carbonaceous species from post-harvest agricultural-waste burning in source region of the Indo-Gangetic Plain. *Tellus B.* 66. <https://doi.org/10.3402/tellusb.v3466.21026>.
- Rajput, P., Sarin, M.M., Sharma, D., Singh, D., 2014b. Organic aerosols and inorganic species from post-harvest agricultural-waste burning emissions over northern India: impact on mass absorption efficiency of elemental carbon. *Environ. Sci.: Process. Impacts.* 16, 2371–2379. <https://doi:10.1039/C4EM00307A>.
- Ram, K., Sarin, M.M., Tripathi, S.N., 2010. A 1 year record of carbonaceous aerosols from an urban site in the Indo-Gangetic Plain: Characterization, sources, and temporal variability. *J. Geophys. Res. Atmos.* 115. <https://doi.org/10.1029/2010JD014188>.
- Ram, K., Sarin, M., 2015. Atmospheric carbonaceous aerosols from Indo-Gangetic Plain and Central Himalaya: Impact of anthropogenic sources. *J. Environ. Manag.* 158, 153-163. <https://doi.10.1016/j.jenvman.2014.08.015>.

- Ram, K., Sarin, M.M., Tripathi, S.N., 2010. A 1 year record of carbonaceous aerosols from an urban site in the Indo-Gangetic Plain: Characterization, sources, and temporal variability. *J. Geophys. Res. Atmosphere*. 115, D24. [https://doi: 10.1029/2010JD014188](https://doi.org/10.1029/2010JD014188).
- Ram, K., Sarin, M.M., Sudheer, A.K., Rengarajan, R., 2012. Carbonaceous and secondary inorganic aerosols during wintertime fog and haze over urban sites in the Indo-Gangetic Plain. *Aerosol and Air Quality Research* 12 (3), 355-366. <https://doi.org/10.4209/aaqr.2011.07.0105>.
- Ramachandran, S., 2005. Aerosol radiative forcing over Bay of Bengal and Chennai: Comparison with maritime, continental, and urban aerosol models. *J. Geophys. Res.* 110, D21206. [https://doi: 10.1029/2005JD005861](https://doi:10.1029/2005JD005861).
- Ramanathan, V., Crutzen, P.J., Kiehl, J.T., Rosenfeld, D., 2001. Aerosols, climate and the hydrological cycle. *Science*. 294, 2119-2124. <https://doi:10.1126/science.1064034>.
- Rao, B.M., and Niranjana, K. 2012. Optical properties of the South Asian winter haze at a tropical coastal site in India. *Atmos. Environ.* 54, 449-455. <https://doi.org/10.1016/j.atmosenv.2012.02.016>
- Rastogi, N., Sarin, M.M., 2006. Chemistry of aerosols over a semi-arid region: evidence for acid neutralization by mineral dust. *Geophys. Res. Lett.* 33. <https://doi.org/10.1029/2006GL027708>.
- Rastogi, N., Singh, A., Sarin, M.M., Singh, D., 2015. Temporal Variability of Primary and Secondary Aerosols over Northern India: Impact of Biomass Burning Emissions. *Atmos. Environ.* 1-8. <http://dx.doi.org/10.1016/j.atmosenv.2015.06.010>.
- Rengarajan, R., Sarin, M.M., Sudheer, A.K., 2007. Carbonaceous and inorganic species in atmospheric aerosols during wintertime over urban and high-altitude sites in North India. *J. Geophys. Res.: Atmospheres*. 112, D21307. <http://doi:10.1029/2006JD008150>.
- Salam, A., Bauer, H., Kassin, K., Ullah, S.M., Puxbaum, H., 2003. Aerosol chemical characteristics of a mega-city in Southeast Asia (Dhaka-Bangladesh). *Atmos. Environ.* 37 (18), 2517-2528. [https://doi.org/10.1016/S1352-2310\(03\)00135-3](https://doi.org/10.1016/S1352-2310(03)00135-3).
- Sarma, V. V. S. S., Krishna, M.S., Paul, Y.S., Murthy, V.S.N., 2015. Observed changes in ocean acidity and carbon dioxide exchange in the coastal Bay of Bengal - a link to air pollution. *Tellus B*. 67, 24638. <https://doi.org/10.3402/tellusb.v67.24638>.
- Sarma, V.V.S.S., Krishna, M.S., Srinivas, T.N.R., Kumari, V.R., Yadav, K., Kumar, M.D., 2021. Elevated acidification rates due to deposition of atmospheric pollutants in the coastal Bay of Bengal. *Geophys. Res. Lett.* 48 (16), e2021GL095159, <https://doi.org/10.1029/2021GL095159>.
- Satsangi, A., Pachauri, T., Singla, V., Lakhani, A and Kumari, K.M. 2010. Carbonaceous aerosols at a suburban site in Indo-Gangetic Plain. *Indian J Radio and Space Phys.* 39, 218-222.
- Savoie, D.L., Prospero, J.M., 1989. Comparison of oceanic and continental sources of non-sea-salt sulphate over the Pacific Ocean. *Nature*. 339, 685-687. <https://doi.org/10.1038/339685a0>.
- Schott, F. A., McCreary, J. P. Jr., 2001. The monsoon circulation of the Indian Ocean. *Progress in Oceanography*. 51, 1-123. [https://doi:10.1016/S0079-6611\(01\)00083-0](https://doi:10.1016/S0079-6611(01)00083-0).

Seinfeld, J.H., Carmichael, G.R., Arimoto, R., Conant, W.C., Brechtel, F.J., Bates, T.S., Cahill, T.A., Clarke, A.D., Doherty, S.J., Flatau, P.J., Huebert, B.J., Kim, J., Markowicz, K.M., Quinn, P.K., Russell, L.M., Russell, P.B., Shimizu, A., Shinzuka, Y., Song, C.H., Tang, Y., Uno, I., Vogelmann, A.M., Weber, R.J., Woo, J.- H., Zhang, X.Y., 2004. ACE-ASIA: regional climatic and atmospheric chemical effects of asian dust and pollution. *Bull. Am. Meteorol. Soc.* 85, 367–380. <https://doi.org/10.1175/BAMS-85-3-367>.

Sharma, S.K., Mandal, T.K., Saxena, M., Rashmi Sharma, A., Datta, A., Saud, T. 2014. Variation of OC, EC, WSIC and trace metals of PM₁₀ in Delhi, India. *J. Atmos. Sol. Terr. Phys.* 113, 10-22. <https://doi.org/10.1016/j.jastp.2014.02.008>.

Shenoy, D.M., Patil, J.S., 2003. Temporal variations in dimethyl sulphonio-propionate and dimethyl sulphide in the Zuari estuary, Goa (India). *Mar. Environ. Res.* 56(3), 387–402. [https://doi.org/10.1016/s0141-1136\(02\)00337-9](https://doi.org/10.1016/s0141-1136(02)00337-9).

Shenoy, D. M., Kumar, M.D., 2007. Variability in abundance and fluxes of dimethyl sulphide in the Indian Ocean. *Biogeochemistry.* 83, 277–292. <https://doi.org/10.1007/s10533-007-9092-4>.

Singh, A., Rastogi, N., Patel, A., Satish, R.V., Singh, D. 2016. Size-segregated characteristics of carbonaceous aerosols over the north western Indo-Gangetic Plain: Year Round temporal behaviour. *Aerosol and Air Quality Res.* 16, 1615-1624. <https://doi.org/10.4209/aaqr.2016.01.0023>.

Srinivas, B., Sarin, M.M., Sarma, V.V.S.S., 2011. Atmospheric dry deposition of inorganic and organic nitrogen to the Bay of Bengal: Impact of continental outflow. *Mar. Chem.* 127, 170-179. <https://doi.org/10.1016/j.marchem.2011.09.002>.

Srinivas, B., Sarin, M., 2012. Atmospheric pathways of phosphorous to the Bay of Bengal: contribution from anthropogenic sources and mineral dust. *Tellus B.* 64. <https://doi.org/10.3402/tellusb.v64i0.17174>.

Srinivas, B., Sarin, M.M., 2013. Atmospheric dry-deposition of mineral dust and anthropogenic trace metals to the Bay of Bengal. *J. Mar. Sys.* 126(0), 56-68. <https://dx.doi.org/10.1016/j.jmarsys.2012.11.004>.

Srinivas, B., Sarin, M.M., 2013. Light absorbing organic aerosols (brown carbon) over the tropical Indian Ocean: impact of biomass burning emissions. *Environ. Res. Lett.* 8, 044042. <http://dx.doi.org/10.1088/1748-9326/8/4/044042>.

Srinivas, B., Sarin, M.M., 2014. PM_{2.5}, EC and OC in atmospheric outflow from the Indo-Gangetic Plain: temporal variability and aerosol organic carbon-to-organic mass conversion factor. *Sci. Total Environ.* 487, 196. <https://doi.org/10.1016/j.scitotenv.2014.04.002>.

Srinivas, B., Sarin, M.M., Rengarajan, R., 2014. Atmospheric transport of mineral dust from the Indo-Gangetic Plain: temporal variability, acid processing, and iron solubility. *G-cubed.* 15, 3226-3243. <https://doi.org/10.1002/2014GC005395>.

Srinivas, B., Kawamura, K., Sarin, M., 2017. Secondary Organic Aerosol Formation over Coastal Ocean: Inferences from Atmospheric Water-Soluble Low Molecular Weight Organic Compounds. *Environ. Sci. Technol.* 51, 4347-4357. <https://doi.org/10.1021/acs.est.6b05986>.

Stein, A., Draxler, R., Rolph, G., Stunder, B., Cohen, M., Ngan, F., 2015. NOAA's HYSPLIT atmospheric transport and dispersion modeling system. *Bull. Am. Meteorol. Soc.* 96, 2059–2077. <https://doi.org/10.1175/BAMS-D-14-00110.1>.

Sudheer, A.K., Sarin, M.M., 2008. Carbonaceous aerosols in MABL of Bay of Bengal: influence of continental outflow. *Atmos. Environ.* 42, 4089–4100. <http://dx.doi.org/10.1016/j.atmosenv.2008.01.033>.

Sullivan, A., Weber, R.J., 2006. Chemical characterization of the ambient organic aerosol soluble in water: 2. Isolation of acid, neutral, and basic fractions by modified size exclusion chromatography. *J. Geophys. Res.* 111, D05315. <https://doi.org/10.1029/2005JD006486>.

Tang, R., Wu, Z., Li, X., Wang, Y., Shang, D., Xiao, Y., Li, M., Zeng, L., Wu, Z., Hallquist, M., Hu, M., Guo, S., 2018. Primary and secondary organic aerosols in summer 2016 in Beijing. *Atmos. Chem. Phys.* 18 (6), 4055–4068. <https://doi.org/10.5194/acp-18-4055-2018>.

Viana, M., Querol, X., Alastuey, A., Ballester, F., Llop, S., Esplugues, A., Fernandez-Patier, R., Garcia dos Santos, S., Herce, M.D., 2008. Characterising exposure to PM aerosols for an epidemiological study. *Atmos. Environ.* 42 (7), 1552–1568. <https://doi.org/10.1016/j.atmosenv.2007.10.087>.

Ventura, A., Simoes, E.F.C., Almeida, A.S., Martins, R., Duarte, A.C., Loureiro, S., and Duarte, R.M.B.O., 2021. Deposition of aerosols onto upper ocean and their impacts on marine biota. *Atmosphere*. 12, 684. <https://doi.org/10.3390/atmos12060684>.

Viswanadham, R., Bharathi, M. D., Sarma, V. V. S. S., 2016. Variations in Concentrations and Fluxes of Dimethyl sulfide (DMS) from the Indian Estuaries. *Estuaries and Coasts*. 39, 695–706. <https://doi.org/10.1007/s12237-015-0039-z>.

Weber, R.J., Sullivan, A.P., Peltier, R.E., Russell, A., Yan, B., Zheng, M., de Grouw, J., Warneke, C., Brock, C., Holloway, J.S., Atlas, E.L., Edgerton, E., 2007. A study of secondary organic aerosol formation in the anthropogenic-influenced southern eastern United States. *J. Geophys. Res. Atmospheres*. 112 (13), 1–13. <https://doi.org/10.1029/2007JD008408>.

Wu, C and Yu, J.Z., 2016. Determination of primary combustion source organic carbon-to-elemental carbon (OC/EC) ratio using ambient OC and EC measurements: secondary OC-EC correlation minimization method. *Atmos. Chem. Phys.* 16, 5453–5465. <https://doi.org/10.5194/acp-16-5453-2016>.

Xu, W., Wang, F., Li, J., Tian, L., Jiang, X., Yang, J., Chen, B., 2017. Historical variation in black carbon deposition and sources to Northern China sediments. *Chemosphere*. 172, 242–248. <https://doi.org/10.1016/j.chemosphere.2016.12.155>

Yadav, K., Sarma, V. V. S. S., Rao, D.B., Kumar, M.D., 2016. Influence of atmospheric dry deposition of inorganic nutrients on phytoplankton biomass in the coastal Bay of Bengal. *Mar. Chem.* 187, 25–34. <https://doi.org/10.1016/j.marchem.2016.10.004>.

Yadav, K., Sarma, V. V. S. S., Kumar, M.D., 2019. Spatial and temporal variability in concentration and characteristics of aerosols at Visakhapatnam (east) and Goa (west) coasts of India. *Environ Sci. Pollut. Res.* <https://doi.org/10.1007/s11356-019-06784-6>.

Yadav, K., Rao, V.D., Sridevi, B., and Sarma, V. V. S. S., 2021. Decadal variations in natural and anthropogenic aerosols optical depth over the Bay of Bengal: Influence of pollutants from Indo-Gangetic Plain. *Environ. Pollu. Science Res.* 28, 55202-55219. [https://doi: 10.1007/s11356-021-14703-x](https://doi.org/10.1007/s11356-021-14703-x).

Zhang, X.Y., Wang, Y.Q., Niu, T., Zhang, X.C., Gong, S.L., Zhang, Y.M., Sun, J.Y., 2012. Atmospheric aerosol compositions in China: spatial/temporal variability, chemical signature, regional haze distribution and comparisons with global aerosols. *Atmos. Chem. Phys.* 12 (2), 779-799. <https://doi.org/10.5194/acp-12-779-2012>.

Table 1: Summary of the data (mean±standard deviation, sd) of the chemical components of TSP collected over the coastal BoB.

Components	Concentrations ($\mu\text{g}\cdot\text{m}^{-3}$)	
	Range	Average±sd
TSP	8.8-177.4	75.3±5.45
Air temperature	23.04-33.38	28.8± 0.39
Relative Humidity	38.67-91.72	73.5±1.39
Na ⁺	1.70-9.28	4.57±2.21
NH ₄ ⁺	0.06-9.27	2.94±0.61
K ⁺	0.21-2.92	1.26±0.17
Mg ²⁺	0.26-0.86	0.50±0.04
Ca ²⁺	0.73-9.73	2.88±0.48
F ⁻	0.01-0.42	0.27±0.02
Cl ⁻	1.99-6.26	4.42±0.63
NO ₃ ⁻	0.87-4.50	2.50±0.16
SO ₄ ²⁻	9.26-44.33	22.0±3.66
nss-SO ₄ ²⁻	8.55-42.44	20.8±2.59
Anthropogenic SO ₄ ²⁻	7.65-37.99	18.7±4.42
MSA	0.06-0.29	0.15±0.05
Biogenic SO ₄ ²⁻	0.90-4.46	2.19±0.17
nss-K ⁺	0.02-0.81	0.27±0.16
nss-Ca ²⁺	0.38-2.76	1.88±0.48
OC	2.86-24.12	12.2±0.68
EC	0.40-4.76	1.92±0.13
OC/EC	2.89-15.75	7.09±0.41
WSOC	2.57-7.18	4.59± 0.13
WIOC	0.29-17.58	7.70 ±0.57
WSOC/OC	0.25-0.90	0.42±0.02
WIOC/EC	0.49-10.77	4.17±0.32
nss-K ⁺ /OC	0.01-0.05	0.02±0.01
nss-K ⁺ /EC	0.01-0.38	0.14±0.11
nss-SO ₄ ²⁻ /EC	5.72-19.73	11.4±1.14
NH ₄ ⁺ /SO ₄ ²⁻ (eq)	0.02-0.87	0.38±0.08
NO ₃ ⁻ /anthSO ₄ ²⁻	0.08-0.23	0.15±0.02
nss-SO ₄ ²⁻ /nss-Ca ²⁺	0.06-54.70	15.2±3.21
nss-K ⁺ /nss-Ca ²⁺	0.02-0.56	0.05±0.02
EC/TSP	0.01-0.09	0.03±0.02
NH ₄ ⁺ /nss-SO ₄ ²⁻	0.02-0.87	0.38±0.2

Table 2: Summary of regression equations, coefficient and their significance with different parameters in the aerosols in the study region

Relation	Regression equation	r ²	p-value
TSP vs EC	EC=0.013TSP + 0.93	0.29	0.001
OC vs EC (Mar-Sep)	OC=3.68EC+3.46	0.71	0.001
OC vs EC (Oct-Feb)	OC=-2.81EC+21.45	0.44	0.001
OC vs WSOC	WSOC=0.16OC+2.66	0.87	0.001
EC vs WIOC (Mar-Sep)	WIOC=3.86EC-0.37	0.58	0.001
EC vs WIOC (Oct-Feb)	WIOC=-2.13EC+15.66	0.35	0.001
EC vs nss-SO ₄ ²⁻	EC=0.045nss-SO ₄ ²⁻ + 0.91	0.32	0.001
WSOC vs WIOC	WIOC=4.37WSOC-12.63	0.79	0.001
AT vs WSOC	WSOC=0.28AT+12.45	0.65	0.001
RH vs WSOC	WSOC=0.05WSOC+7.85	0.42	0.001
Na ⁺ vs Cl ⁻ +(nss-SO ₄ ²⁻ +NH ₄ ⁺)	Cl ⁻ +(nss-SO ₄ ²⁻ +NH ₄ ⁺)=1.19Na ⁺ +28.6	0.85	0.001
Na ⁺ vs Mg ²⁺	Mg ²⁺ =0.08Na ⁺ + 22.6	0.40	0.001
nss-SO ₄ ²⁻ vs NH ₄ ⁺ (Mar-Sep)	1.76NH ₄ ⁺ +7.71	0.81	0.001
nss-SO ₄ ²⁻ vs NH ₄ ⁺ (Oct-Feb)	0.70NH ₄ ⁺ + 121.2	0.81	0.001

Legend to Figures:

Figure 1: Monthly mean variability in aerosol optical depth (AOD; color scale), direction of the wind (shown as arrows) and weekly mean HYSPLIT air-mass trajectories to the study site.

Figure 2: Monthly mean variations in a) total suspended particulate matter (TSP) and b) ionic composition in the TSP.

Figure 3: Monthly mean variations in concentrations of ionic and carbonaceous components in the TSP over the coastal BoB.

Figure 4: The monthly mean percentage contribution of different ions to total ions concentrations in the TSP over the coastal BoB.

Figure 5: Relationship between a) EC and OC, b) OC and WSOC, c) EC and WISOC and d) WSOC and WISOC in the TSP over the coastal BoB. The blue closed circles represent data from March to September whereas the red circles represent from winter.

Figure 6: Monthly mean variations in diagnostic binary ratios of ionic and carbonaceous components in the TSP.

Figure 7: The monthly mean variations in a) ratio of neutralization potential to acidic potential and b) total hydrogen ion concentration in the TSP.

Figure 8: Monthly mean variations in a) MSA, b) biogenic SO_4^{2-} , c) anthropogenic SO_4^{2-} and contribution of biogenic SO_4^{2-} to total SO_4^{2-} in the TSP.

Figure 1:

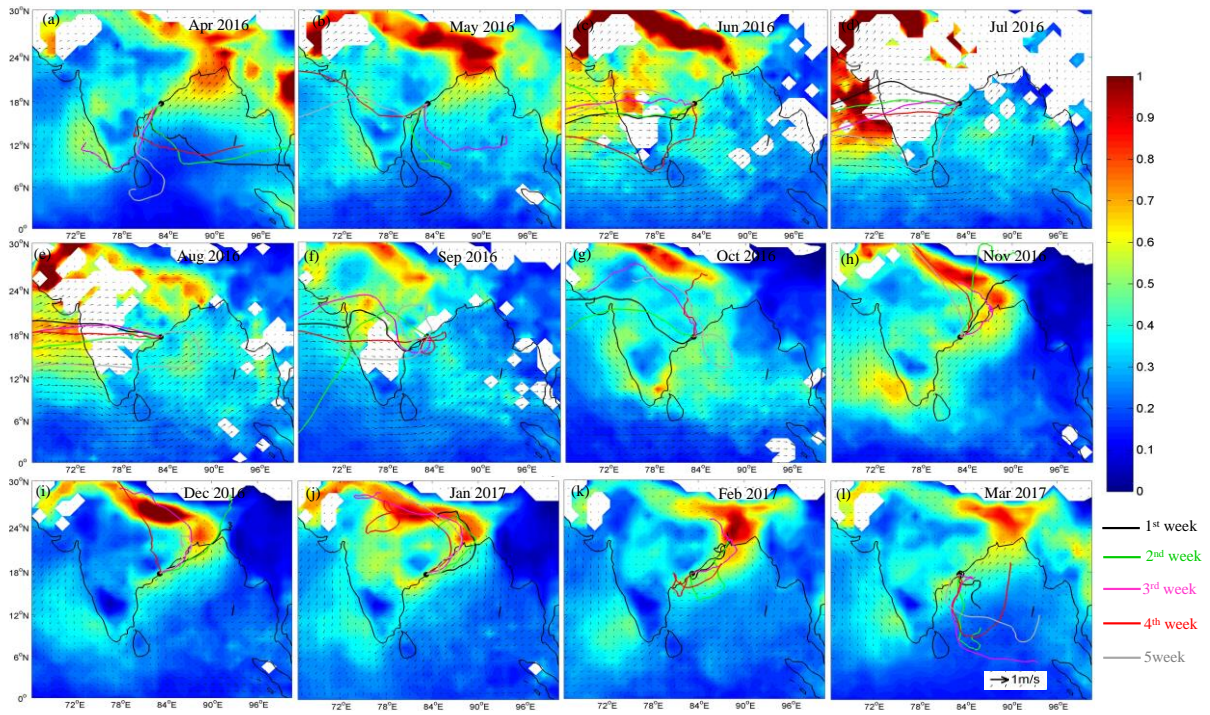


Figure 2:

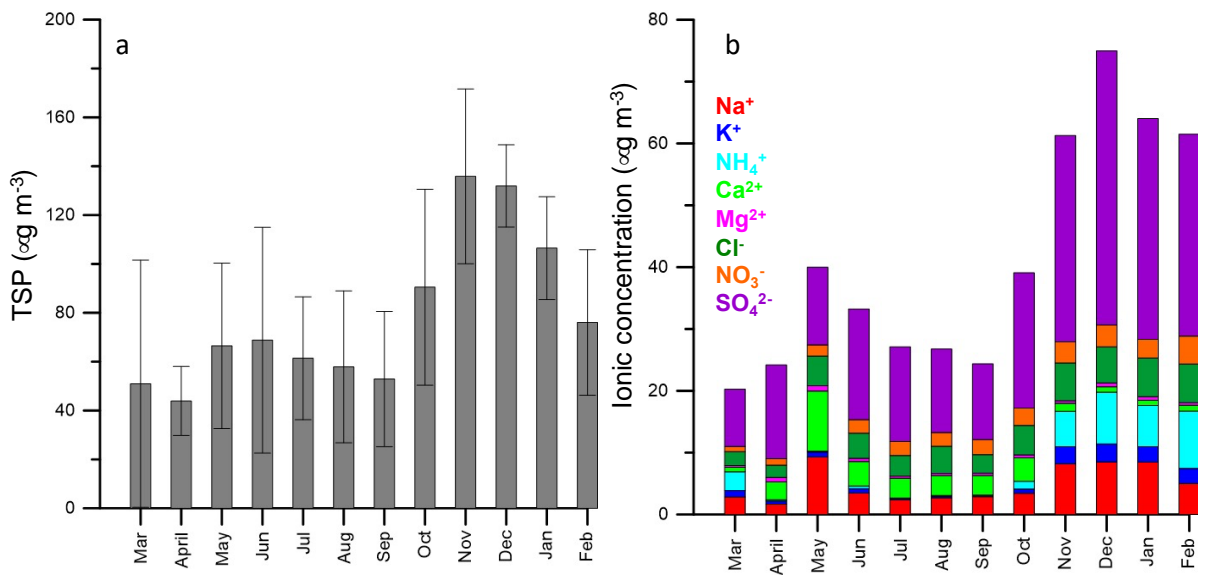


Figure 3:

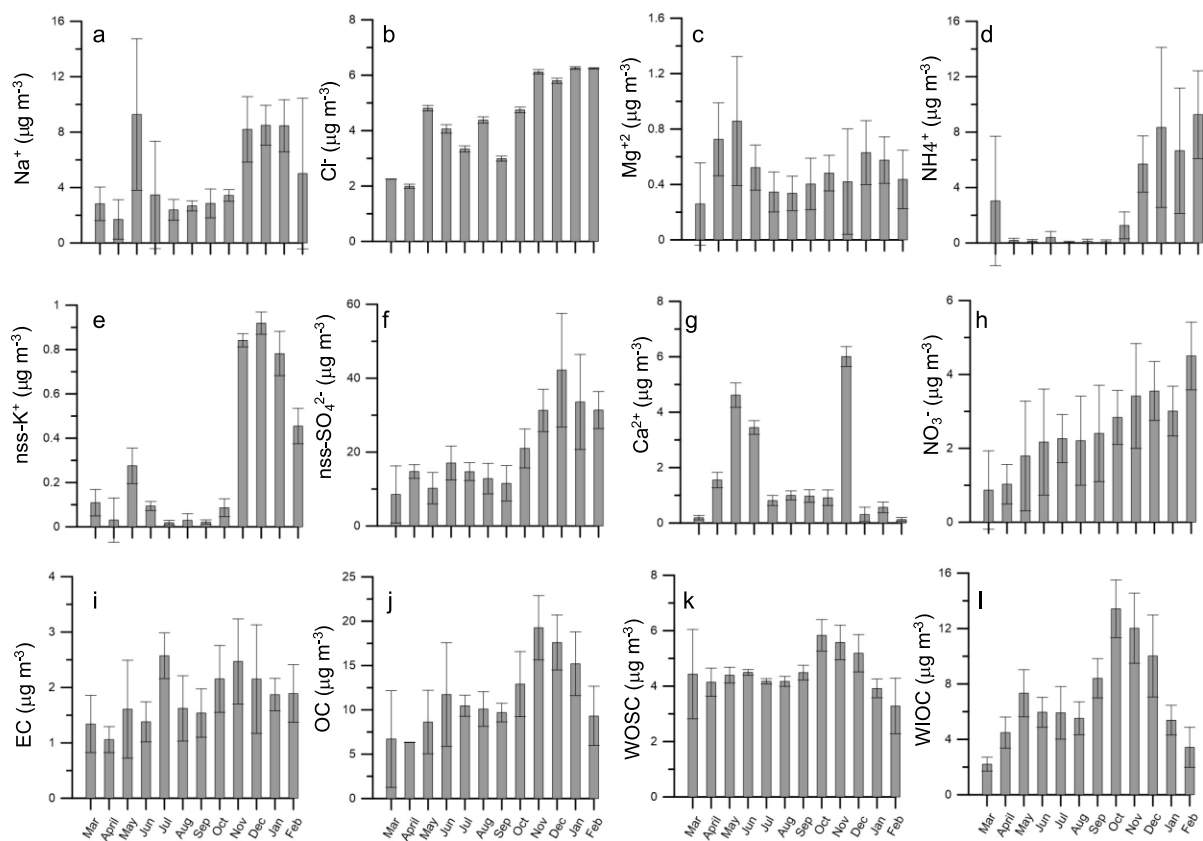


Figure 4:

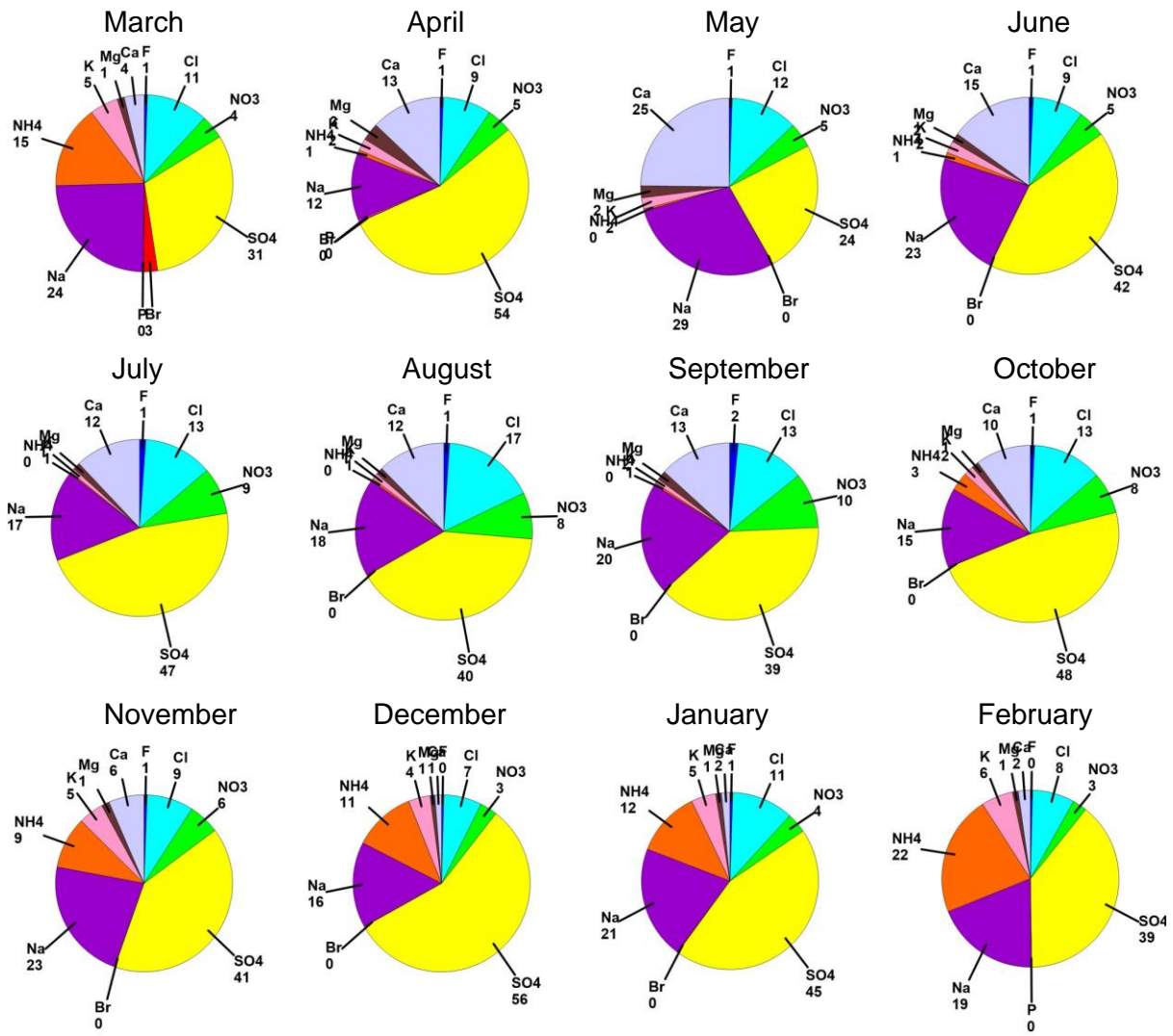


Figure 5:

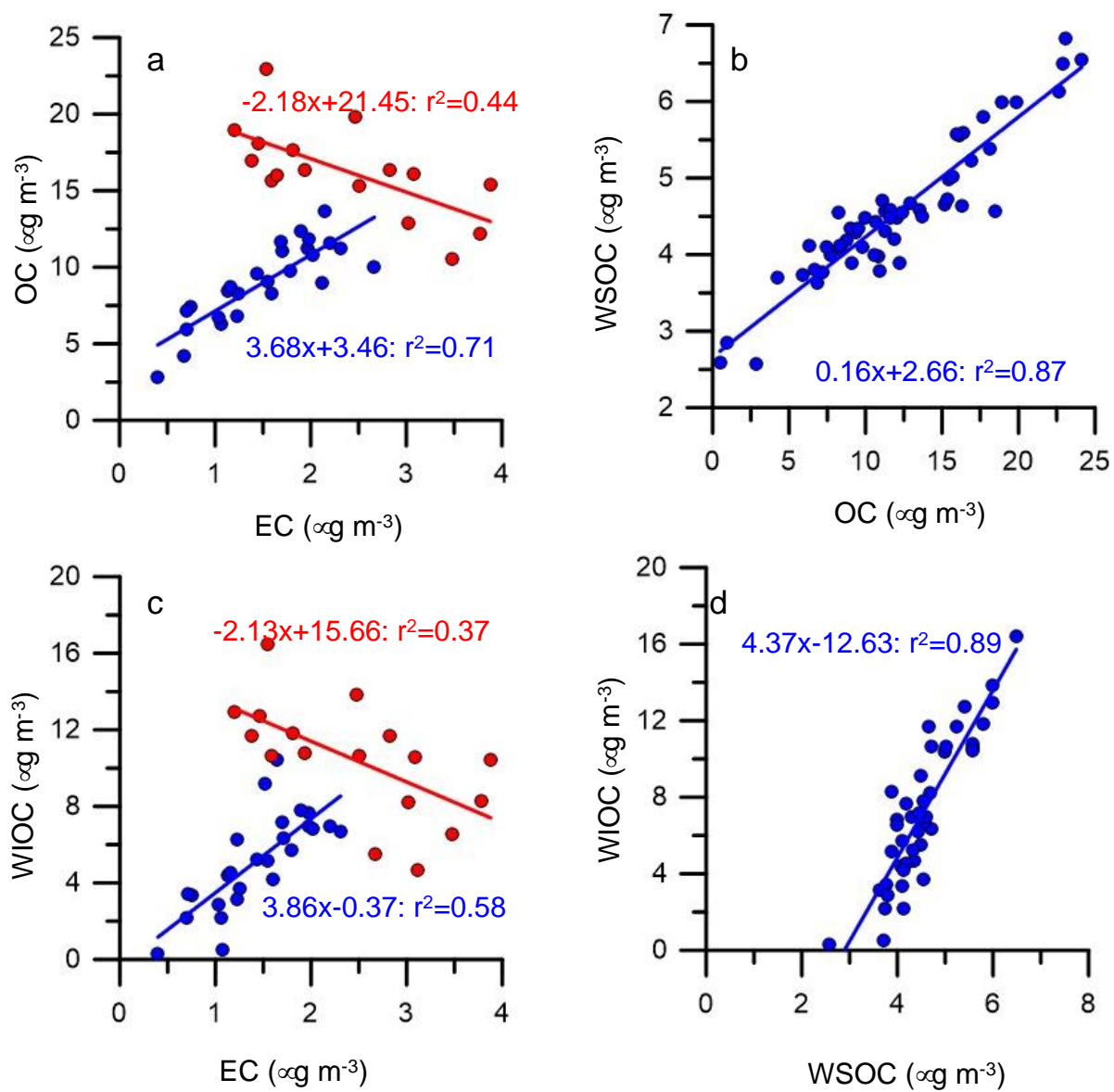


Figure 6:

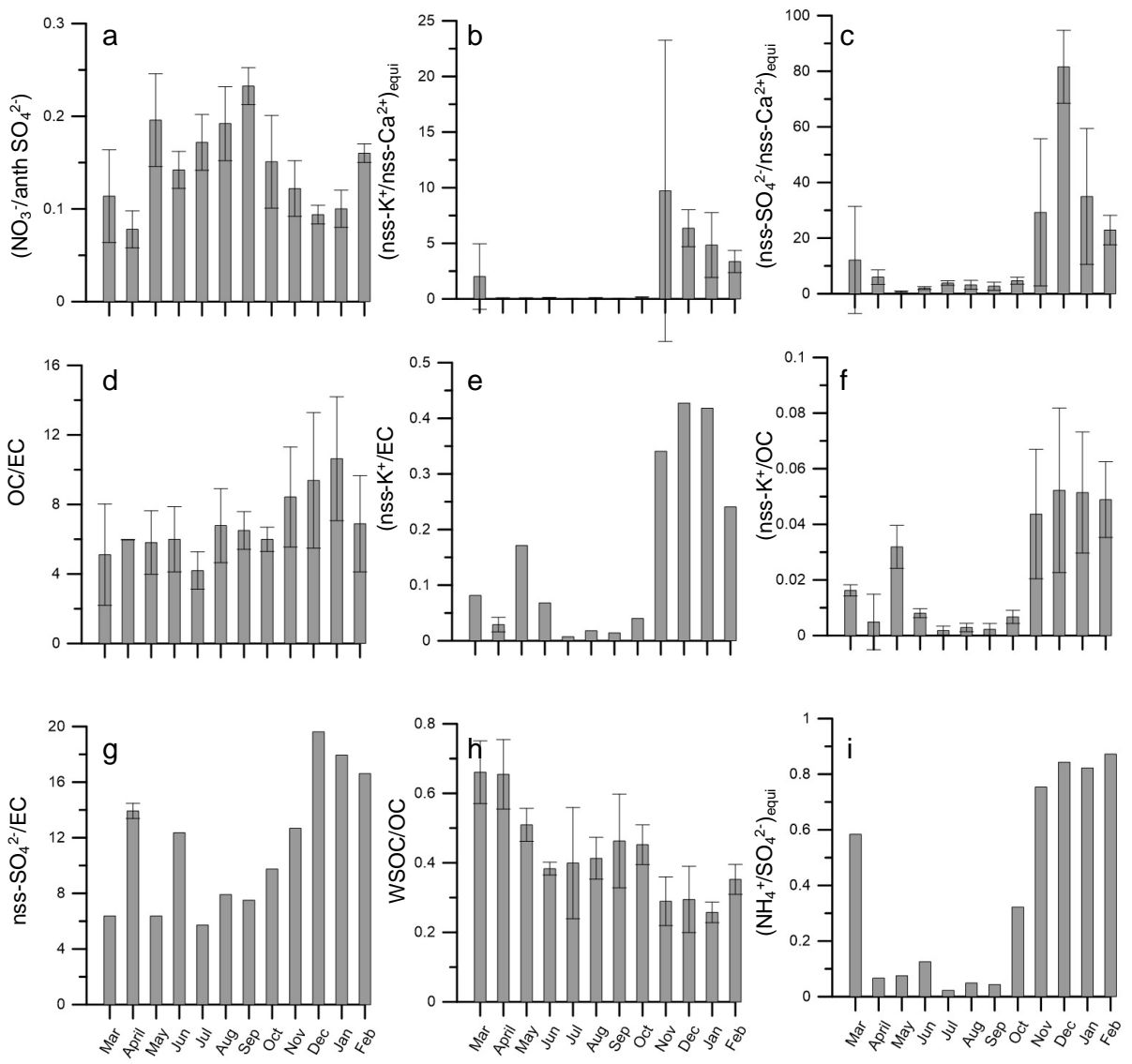


Figure 7:

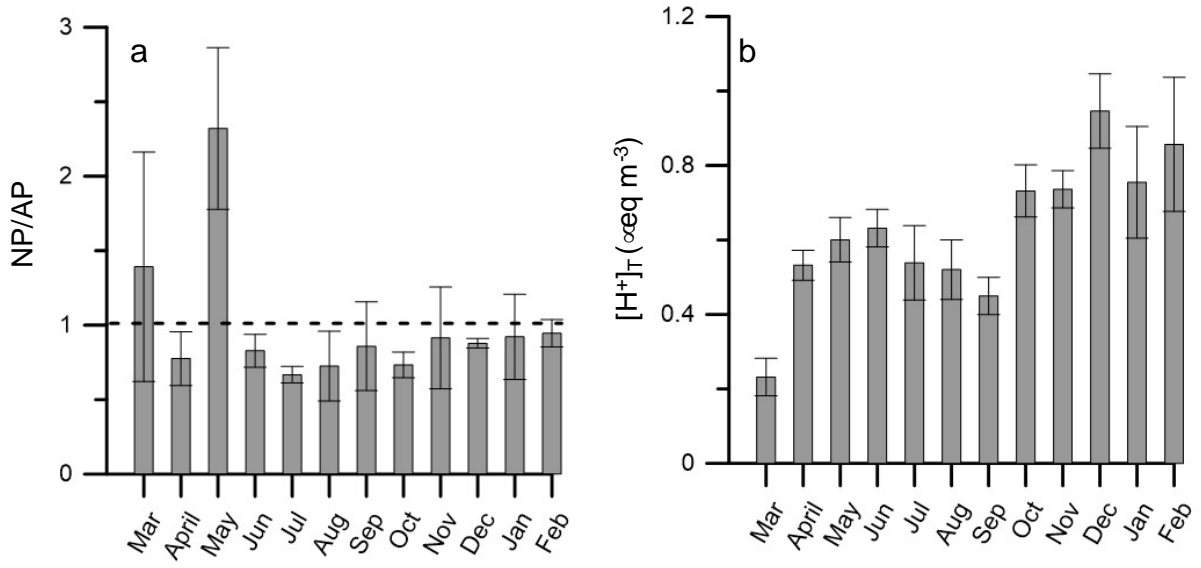
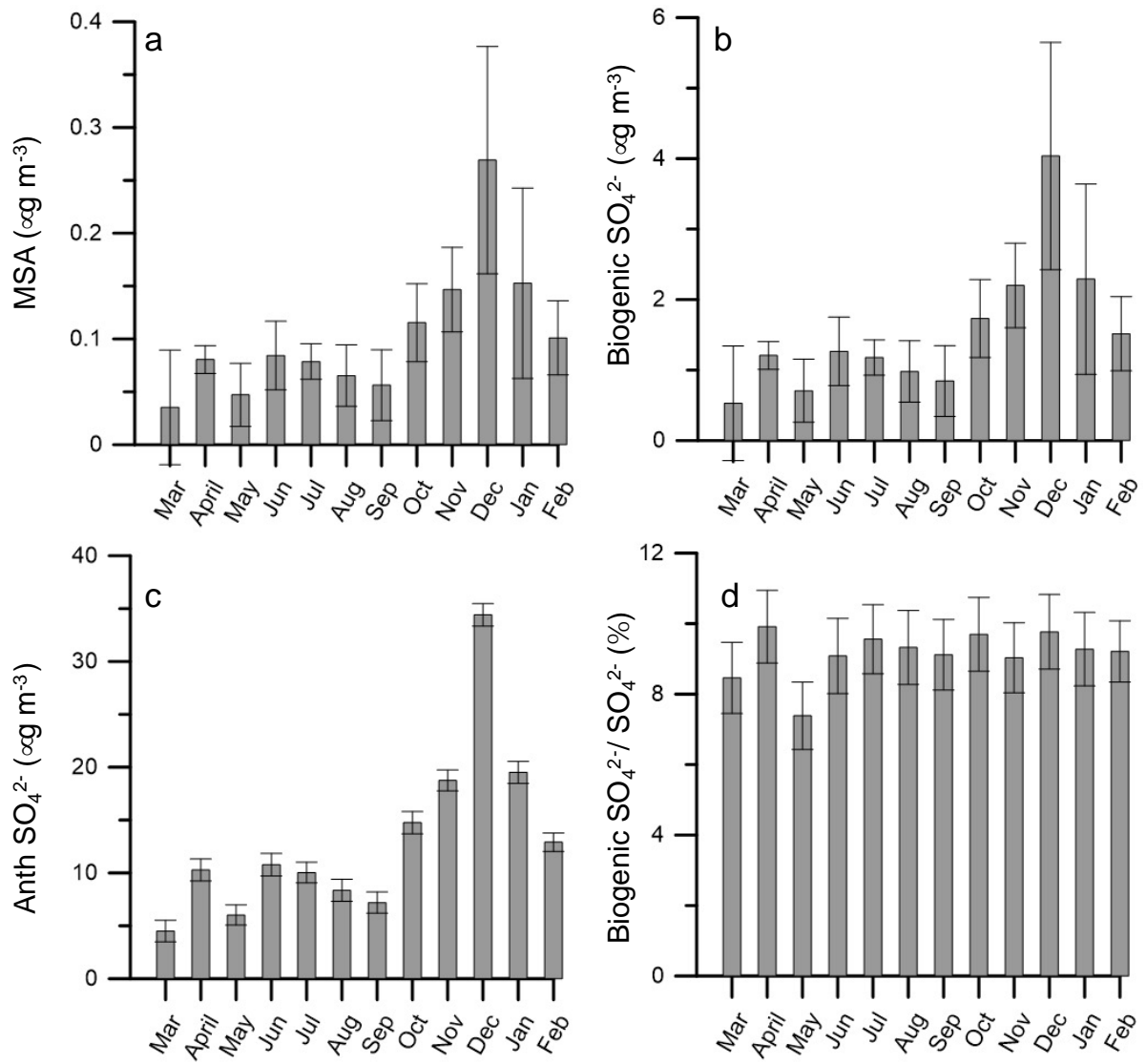
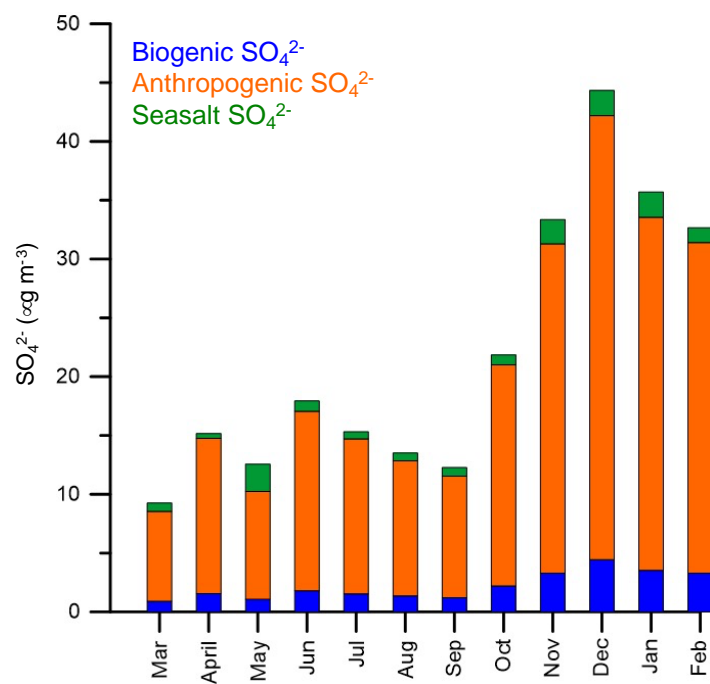


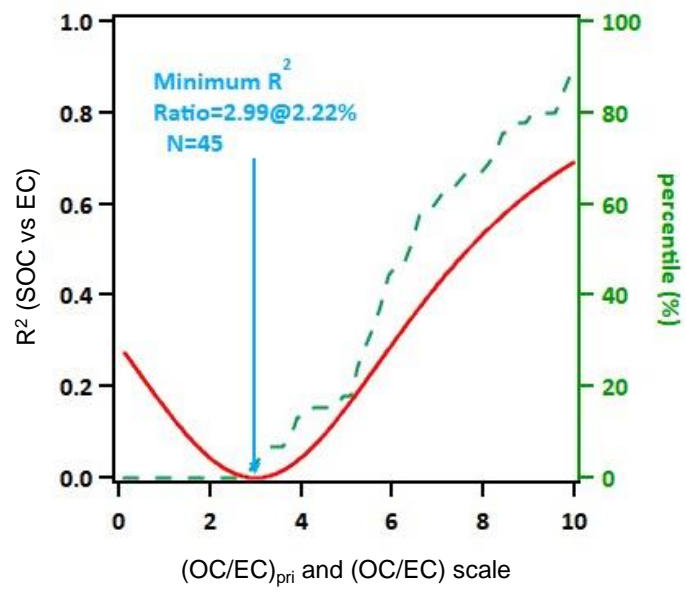
Figure 8:



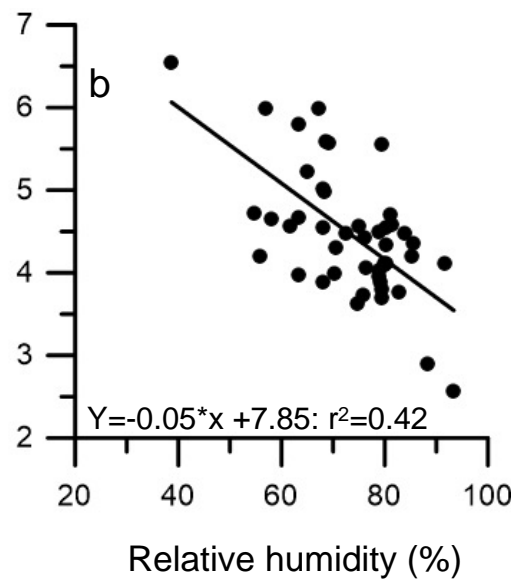
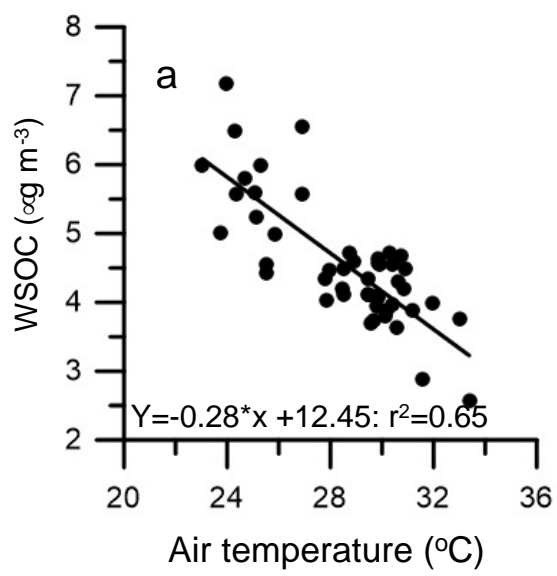
Supplementary Figure S1: Monthly variations in biogenic, anthropogenic and sea-salt SO_4^{2-} concentrations in the TSP over the coastal BoB.



Supplementary Figure S2: Estimation of primary OC/EC ratio from emissions using MRS method over the coastal Bay of Bengal.



Supplementary Figure S3: The relationship of WSOC with a) air temperature and b) relative humidity.



Supplementary Table T1: Mean (\pm standard deviation) of diagnostic binary ratios during winter and other seasons in the study region

Diagnostic ratio	Winter	Other seasons
nss-K ⁺ /nss-Ca ²⁺	5.3 \pm 3	0.06 \pm 0.02
nss-SO ₄ ²⁻ /nss-Ca ²⁺	36.2 \pm 26	3.3 \pm 2
OC/EC	8.8 \pm 1.6	5.8 \pm 0.8
nss-K ⁺ /EC	0.4 \pm 0.1	0.05 \pm 0.01
nss-K ⁺ /OC	0.06 \pm 0.01	0.01 \pm 0.01
nss-SO ₄ ²⁻ /EC	16.6 \pm 4	8.7 \pm 3
WSOC/OC	0.32 \pm 0.1	0.5 \pm 0.1
WIOC/EC	3.9 \pm 2	3.3 \pm 0.6